pTAC2, -6, and -12 Are Components of the Transcriptionally Active Plastid Chromosome That Are Required for Plastid Gene Expression

Jeannette Pfalz,[a] Karsten Liere,[b] Andrea Kandlbinder,[c] Karl-Josef Dietz,[c] and Ralf Oelmüller[a,1]

[a] Institute of General Botany and Plant Physiology, Friedrich-Schiller-University, 07743 Jena, Germany
[b] Institute of Biology (Genetics), Humboldt University, D-10115 Berlin, Germany
[c] Department of Plant Physiology and Biochemistry, University of Bielefeld, 33501 Bielefeld, Germany

Transcription in plastids is mediated by a plastid-encoded multimeric (PEP) and a nuclear-encoded single-subunit RNA polymerase (NEP) and a still unknown number of nuclear-encoded factors. By combining gel filtration and affinity chromatography purification steps, we isolated transcriptionally active chromosomes from *Arabidopsis thaliana* and mustard (*Sinapis alba*) chloroplasts and identified 35 components by electrospray ionization ion trap tandem mass spectrometry. Eighteen components, called plastid transcriptionally active chromosome proteins (pTACs), have not yet been described. T-DNA insertions in three corresponding genes, *ptac2, -6,* and *-12*, are lethal without exogenous carbon sources. Expression patterns of the plastid-encoded genes in the corresponding knockout lines resemble those of Δ*rpo* mutants. For instance, expression of plastid genes with PEP promoters is downregulated, while expression of genes with NEP promoters is either not affected or upregulated in the mutants. All three components might also be involved in posttranscriptional processes, such as RNA processing and/or mRNA stability. Thus, pTAC2, -6, and -12 are clearly involved in plastid gene expression.

INTRODUCTION

Chloroplasts of higher plants possess at least two RNA polymerases with different biochemical properties and phylogenetic origins: a plastid-encoded multimeric RNA polymerase (PEP), which resembles eubacterial RNA polymerases, and a nucleus-encoded phage-type RNA polymerase (NEP) (Hu and Bogorad, 1990; Igloi and Kössel, 1992; Lerbs-Mache, 1993; Pfannschmidt and Link, 1994; Liere and Maliga, 1999). In addition to PEP, the existence of NEP has already been suggested from studies with the parasite *Epifagus virginiana*, which lacks the plastid *rpoBC* operon (Morden et al., 1991). Similar results were obtained for the plastid ribosome–deficient barley (*Hordeum vulgare*) mutant *albostrians* (Hess et al., 1993) and tobacco (*Nicotiana tabacum*) *rpo* deletion mutants (Allison et al., 1996; Hajdukiewicz et al., 1997), both still synthesizing plastid transcripts. NEP genes have been identified in the genome of many plant species (Hedtke et al., 1997; Weihe et al., 1997; Young et al., 1998; Ikeda and Gray, 1999). *Arabidopsis thaliana* contains three NEPs: RpoTm is located in mitochondria, while RpoTmp and RpoTp are found in plastids (Hedtke et al., 1997, 2000; Liere et al., 2004). RpoTmp is also imported into mitochondria, suggesting a dual function in organellar transcription (Hedtke et al., 2000). NEP genes for plastid proteins might

have derived from a gene duplication event of a mitochondrial phage-type RNA polymerase gene (Hedtke et al., 1997).

NEP preferentially transcribes housekeeping genes, while PEP is predominantly involved in the transcription of photosynthesis genes (Allison et al., 1996; Hajdukiewicz et al., 1997). However, in PEP-deficient mutants, spurious transcripts initiated by NEP cover the entire plastome. Besides selective promoter utilization, the transcript pattern of plastids is also determined by transcript stability (Krause et al., 2000; Legen et al., 2002), whereas the RNA stability itself seems to depend on the type of the generating RNA polymerase (Cahoon et al., 2004).

While the subunits $\alpha\beta\beta'\beta''$ of the core complex of PEP are plastid encoded, the specificity of the holoenzyme ($\alpha\beta\beta'\beta''\sigma$) is determined by nuclear-encoded sigma factors (Tiller et al., 1991; Homann and Link, 2003; Suzuki et al., 2004). They are expressed in a light-dependent, developmental, and tissue-specific manner (Allison, 2000; Kasai et al., 2004; Ishizaki et al., 2005). Based on the promoter structures, three classes of plastid genes can be distinguished: class I genes are preferentially transcribed by PEP, class II genes by NEP, and class III genes by both polymerases (Hajdukiewicz et al., 1997; Ishizaki et al., 2005).

Many attempts have been made to identify nuclear-encoded proteins involved in plastid transcription and translation. Subunits of the PEP core are present in two plastid protein preparations, the transcriptionally active chromosome (TAC) and the soluble RNA polymerase (sRNAP). The TAC is membrane attached and consists of several multimeric protein complexes. In in vitro assays, the TAC can transcribe endogenously bound DNA, while the transcriptional activity of sRNAP requires the addition of DNA (Igloi and Kössel, 1992; Krause et al., 2000). TAC fractions have been isolated by gel filtration from different organisms (Briat et al., 1979; Rushlow and Hallick, 1982; Reiss

and Link, 1985). The specific activity of the isolated complexes depends on the purification procedure (Suck et al., 1996; Krause et al., 2000). Initially, it was believed that sRNAP transcribes preferentially tRNA genes, while TAC is involved in rRNA transcription (Gruissem et al., 1983; Narita et al., 1985); however, run-on transcription assays uncovered that both highly purified fractions transcribed rRNA, tRNA, and plastid protein-coding genes (Reiss and Link, 1985; Rajashekar et al., 1991; Krupinska and Falk, 1994). Finally, TAC and sRNAP preparations from proplastids, chloroplasts, and etioplasts have different protein compositions, demonstrating their dynamics in response to environmental and developmental changes (Reiss and Link, 1985; Pfannschmidt and Link, 1994; Suck et al., 1996).

Forty to sixty polypeptides appear to be present in the TAC from chloroplasts, along with two core subunits of PEP and ETCHED1 (ET1) with high homology to the nuclear transcription elongation factor TFSII (Suck et al., 1996; Krause and Krupinska, 2000; da Costa e Silva et al., 2004). Together with the findings that the *ET1-R* mutants exhibit quantitative, but no qualitative, differences in TAC activity, it was suggested that ET1 may be involved in plastid mRNA elongation (da Costa e Silva et al., 2004). Furthermore, analyses of TAC preparations from ribosome-deficient mutants suggest that the fraction also contains a nuclear-encoded RNA polymerase activity (Suck et al., 1996). Analyses of highly purified sRNAP preparations as well as plastid DNA–bound proteins (nucleoids) led to the identification of additional nuclear-encoded components (Murakami et al., 2000; Pfannschmidt et al., 2000; Chi-Ham et al., 2002; Ogrzewalla et al., 2002; Sekine et al., 2002; Jeong et al., 2003; Loschelder et al., 2004; Suzuki et al., 2004). One of the best-characterized components of sRNAP is the transcription kinase cpCK2, which plays a role in the regulation of plastid gene expression via phosphorylation and redox signaling (Baginsky et al., 1997, 1999; Ogrzewalla et al., 2002). The nucleoid-associated protein MFP1 is a substrate of cpCK2, which inhibits the DNA binding activity of MFP1 by phosphorylation (Jeong et al., 2004). In mature chloroplasts, MFP1 is attached to thylakoids; hence, it may possibly anchor the nucleoids to the thylakoid membranes (Jeong et al., 2003). Other well-characterized proteins in nucleoids are a sulfite reductase, which participates in organellar nucleoid organization (Cannon et al., 1999; Chi-Ham et al., 2002; Sekine et al., 2002), and a DNA binding protein CND41 with aspartic protease activity (Murakami et al., 2000), possibly involved in regulation of senescence (Kato et al., 2004).

We isolated highly purified TACs from *Arabidopsis* and mustard (*Sinapis alba*) and analyzed their protein composition by electrospray ionization ion trap tandem mass spectrometry. Out of 35 identified components, 18 have not yet been described. In this study, we focused on three TAC components: pTAC2, -6, and -12. Interestingly, pTAC2 and pTAC6 are also present in sRNAP fractions, which have eight additional components besides the four PEP core subunits (Suzuki et al., 2004). While pTAC2 encodes a pentatricopeptide repeat–containing protein, the other two components, pTAC6 and pTAC12, contain no known domain and exhibit no homologies that would allow prediction of their function in plastid gene expression. Analyses of the expression of plastid genes in knockout lines suggest that the three TAC components are required for proper function of
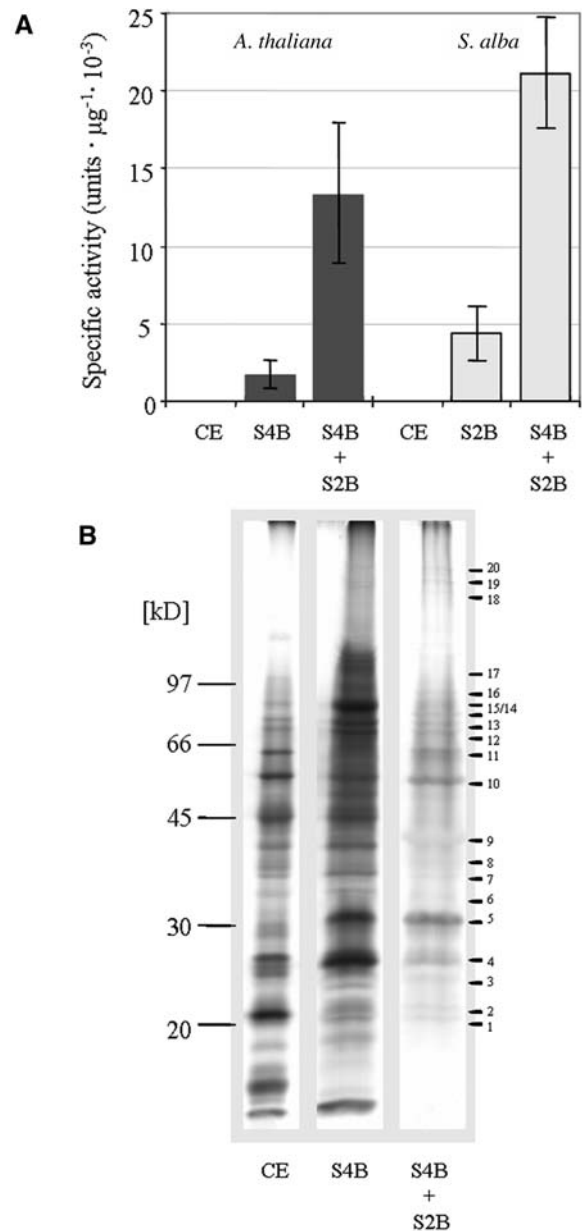

Figure 1. Purification of the *Arabidopsis* and Mustard TAC.

(A) The transcriptional activity of the TAC preparations (representative for at least four independent experiments) from *Arabidopsis* and mustard was measured in the chloroplast lysate, after Sepharose 4B (S4B) and Sepharose 4B plus 2B (S2B) chromatography. The S4B + S2B preparations were used for mass spectrometry. Each point and error bars represent the mean value of three replicate samples and corresponding standard deviation.
(B) SDS-PAGE of TAC preparations from mustard. Lane 1, crude extract of chloroplast (CE, 25 μg); lane 2, after Sepharose 4B (S4B) chromatography; lane 3, after Sepharose 4B and 2B (S4B + S2B) chromatography. Proteins corresponding to equal TAC activity were loaded on lanes 2 and 3. The gel was stained with silver. Mass markers in kilodaltons are at left. Bars at right point to bands that were analyzed by mass spectrometry.

Table 1. Identified Proteins from *Arabidopsis* and Mustard in TAC Preparations

NCBI Acc. No./AGI Acc. No.[a]	Protein	Position[b]	Z[c]	ΔM[d]		x_{corr}[e]	
				Ara	Sin	Ara	Sin
Transcription							
gi|7525065	RNA polymerase α-chain (RpoA)	40–50	2		0.7		2.60
ArthCp055		292–310	2	0.6	1.2	6.62	3.87
		322–328	2	−0.1		2.60	
gi|7525025	RNA polymerase β-chain (RpoB)	13–31	2	−0.2		4.30	
ArthCp014		32–43	2	0.0		3.95	
		276–290	2	0.4	0.0	4.36	3.44
		322–337	2	0.1	0.5	4.98	4.08
		354–386	3		0.7		3.60
		387–397	2	0.7		3.47	
		450–466	2	−0.6		4.11	
		603–621	2	−0.4		3.16	
		643–661	2	−0.2		3.44	
		769–779	2	−0.2		3.06	
		907–917	2	0.1		3.79	
		918–932	2	−1.1		4.64	
		940–957	2	0.3	0.1	3.57	3.87
		993–1017	3	0.0	0.1	4.73	4.04
		1025–1048	2	1.4		2.72	
		1056–1069	2	0.3	0.0	5.12	4.30
gi|7525024	RNA polymerase β′-chain (RpoC1)	12–26	2		0.2		3.26
ArthCp013		173–188	2	1.0		3.34	
		287–297	2	0.4		3.60	
		303–314	2	0.6		3.54	
		327–341	2	0.3		2.69	
		382–394	2	−0.6		3.30	
		434–454	3		0.2		5.21
		461–474	2	0.3	0.9	3.97	3.27
		485–510	3	1.0		3.78	
		596–605	2		1.3		2.72
gi|7525023	RNA polymerase β″-chain (RpoC2)	44–68	2	0.5	0.8	3.30	3.62
ArthCp012		69–84	2	0.3		6.04	
		241–249	2	−0.8	0.1	2.98	2.57
		250–260	2	0.3	−1.2	3.72	2.51
		266–276	2		0.1		4.25
		277–288	2	0.3		2.91	
		307–338	3	−1.0		3.02	
		434–454	3		0.2		5.12
		485–510	3	1.0		3.78	
		526–535	2	0.4		2.07	
		590–608	2	0.7		2.78	
		610–620	2	1.0		2.54	
		720–730	2	1.3	0.1	2.99	2.59
		779–801	2	1.1		3.12	
		810–823	2	−0.6		2.96	
		824–834	2	0.7	−0.3	2.98	3.98
		1152–1162	2	0.0	−1.2	2.61	3.55
		1227–1248	3	0.1		5.12	
		1309–1325	2	0.3		3.92	
		1345–1354	2	0.3		2.92	
DNA replication, DNA topology, DNA binding							
gi|11994141	DNA polymerase A, putative (PolA)	287–302	2	0.3		3.92	
At3g20540		322–337	2	0.3		3.24	
		342–356	2	0.6		4.12	
		377–391	2	0.5		4.11	
		448–466	2	−1.1		2.72	
gi|15228353	DNA gyrase subunit A, putative (GyrA)	109–125	2	−0.3	−1.6	2.89	2.90

(Continued)

Table 1. (continued).

NCBI Acc. No./AGI Acc. No.[a]	Protein	Position[b]	Z[c]	ΔM[d] Ara	ΔM[d] Sin	x_{corr}[e] Ara	x_{corr}[e] Sin
At3g10690		194–201	1	0.7		2.19	
		220–248	3	0.0		4.52	
		352–365	2	−0.9		3.91	
		405–417	2	0.6		3.79	
		444–453	2	−0.8		2.85	
		535–548	2	0.6	0.7	4.22	3.97
		562–571	2	−1.6	−1.1	2.90	3.21
		675–692	2	−1.7		3.91	
gi|15228245	DNA gyrase subunit B, putative (GyrB)	368–394	3	−0.4		3.61	
At3g10270		484–499	2	−1.6	−0.8	5.81	4.75
Translation							
gi|15237059	Elongation factor Tu (EF-Tu)	127–142	2		0.5		4.22
At4g20360		205–222	2		0.5		2.97
		283–301	2	−0.1	−0.1	4.42	3.19
		316–326	2	0.4	0.1	3.44	3.07
		342–357	2		−0.2		3.53
gi|15232274	Ribosomal protein L12-1	69–82	2		0.3		4.57
At3g27830		83–91	2		0.6		2.87
gi|5881732	Ribosomal protein S3	68–82	2		0.0		4.89
ArthCp061		92–101	2		0.5		3.61
		148–158	2		−0.2		4.19
		159–167	2		0.6		3.26
		184–192	1		0.4		1.71
gi|15238369	Ribosomal protein L29	74–86	2		−0.1		2.82
At5g65220		97–103	1		1.2		1.68
Detoxification, protein modification							
gi|15241373	Iron superoxide dismutase (FE-SOD1)	92–113	2	0.6		5.80	
At5g51100		155–165	2	0.0		3.77	
		168–184	2	1.1		4.03	
		188–199	2	−0.8	0.2	4.28	3.67
		210–241	3	−0.4	0.9	4.72	4.2
		243–252	2	0.0		3.15	
		253–262	2	0.3	0.0	2.97	3.17
gi|11358867	Iron superoxide dismutase (FE-SOD3)	96–106	2	0.7		3.33	
At5g23310		145–161	3	−1.5		3.83	
		228–245	3	−1.5		3.68	
gi|15230779	Thioredoxin, putative	80–90	2	0.5	−1.0	3.58	3.41
At3g06730		132–142	2	0.3	0.4	3.14	3.40
		166–183	2	0.8		2.91	
		188–199	2		0.1		3.65
Metabolism							
gi|15222232	pfkB-type carbohydrate kinase family protein (PFKB1)	89–119	3	−1.5		4.75	
At1g69200		227–235	2	0.7		2.66	
		334–342	2	0.1		2.87	
		396–412	2	0.6		4.20	
		437–454	2	0.8		3.96	
		490–504	2	1.1	0.4	2.80	4.23
		505–516	2	0.6	−0.6	3.22	2.52
		601–614	2	0.5		3.83	
gi|15232415	pfkB-type carbohydrate kinase family protein (PFKB2)	146–160	3		−0.5		3.05
At3g54090		223–240	2	−0.8		3.46	
		327–341	2	0.6		4.32	
		364–373	2	0.0		3.04	
		401–413	2		−0.5		3.93
gi|15222509	Mur ligase family protein	213–231	2	0.2		3.34	

(Continued)

Table 1. (continued).

NCBI Acc. No./AGI Acc. No.[a]	Protein	Position[b]	Z[c]	ΔM[d] Ara	ΔM[d] Sin	x_{corr}[e] Ara	x_{corr}[e] Sin
At1g63680		252–273	2		−1.5		2.86
		318–338	2	0.3		6.31	
		389–409	2	1.0		3.51	
		746–767	2	−0.1		3.43	
DNA/RNA binding, unknown function							
gi|15223748	PTAC1 (DNA binding protein p24-related)	64–80	2	0.5		3.20	
At1g14410		81–89	2		0.7		2.91
		100–112	2		0.8	2.60	
		138–156	2	0.8		3.36	
		181–199	2	0.2	0.7	3.10	3.99
		200–213	2	0.6		3.64	
		214–247	3	0.1		3.73	
		248–263	2	0.0	−1.4	3.56	2.68
gi|15221411	PTAC2 (pentatricopeptide repeat-containing protein)	57–69	2		0.4		3.15
At1g74850							
		103–113	2	−0.2	0.8	3.77	3.76
		192–201	2	0.3	−0.5	3.37	3.18
		224–239	2	0.6		4.20	
		718–740	2	0.4		2.98	
		741–753	2	0.4		3.48	
gi|15229259	PTAC3 (SAP domain-containing protein)	74–83	2		0.0		3.30
At3g04260		88–109	2	−0.3		4.90	
		178–189	2	0.1		4.59	
		162–171	2		0.9		2.92
		304–319	2	−0.3		3.86	
		353–376	2	1.4		4.77	
		384–395	2	0.4	0.0	4.25	3.01
		414–438	2	0.6		5.10	
		459–479	2	0.8		5.30	
		496–515	2	1.1		3.55	
		547–560	2	0.6		3.43	
		618–631	2	1.0	0.7	4.27	3.82
		703–713	2	1.0		4.30	
gi|18408237	PTAC4 (PspA/IM30 family protein)	84–98	2		0.7		3.10
At1g65260		99–113	2		−0.4		5.19
		116–126	2		0.2		3.54
		146–152	1		0.2		1.71
		166–176	2		0.1		3.47
		167–176	2		−0.5		3.43
		184–194	2		−0.1		3.13
		223–241	2		0.5		5.91
		246–267	2		1.1		5.08
		268–284	3		−0.5		4.35
		313–324	2		0.1		4.58
gi|15236331	PTAC5 (peptidoglycan binding domain-containing protein)	80–92	2	−0.1	−0.6	4.78	4.40
At4g13670		221–229	2		−0.1		2.96
gi|18395008	PTAC6 (expressed protein)	83–112	2	1.1		6.16	
At1g21600		113–129	2	−0.3		3.21	
		149–161	2	1.0		3.06	
		162–177	2	1.1		2.84	
		232–250	2	0.8		5.19	
gi|22327025	PTAC7 (expressed protein)	64–72	2		0.6		2.73
At5g24314		80–91	2	−0.8		4.50	
		96–112	2	0.9		2.80	
		123–131	2		−0.9		2.80
		132–161	2	0.7		4.79	

(Continued)

Table 1. (continued).

NCBI Acc. No./AGI Acc. No.[a]	Protein	Position[b]	Z[c]	ΔM[d] Ara	Sin	x_{corr}[e] Ara	Sin
gi|18407178	PTAC8 (expressed protein)	64–88	2	1.0		4.80	
At2g46820		127–148	2	−0.2		3.96	
gi|18415421	PTAC9 (expressed protein)	121–130	2	1.5	0.0	2.63	3.59
At4g20010		288–299	2		0.7		3.47
gi|15228384	PTAC10 (S1 domain-containing protein)	41–56	2	0.7	−0.4	3.36	4.10
At3g48500		77–93	2	−1.1	0.0	3.87	4.15
		95–114	2	0.2		4.61	
		127–138	2	0.9		3.04	
		194–201	1	0.7		2.19	
		244–252	2	0.2		2.67	
		354–362	2	−0.3		2.69	
		404–424	2	0.6		5.64	
		444–453	2	0.4		3.35	
		468–478	2	0.1		3.86	
		503–515	2	−0.3		4.35	
		532–543	2	0.3	0.4	3.22	3.21
		553–571	2	−0.3		5.68	
gi|15227028	PTAC11 (DNA binding protein p24-related)	69–84	2	0.7		3.02	
At2g02740		81–89	2		0.7		2.91
		96–103	2		0.0		2.58
		104–116	2	0.4	0.4	3.83	3.78
		120–134	2	0.1	−0.6	3.73	4.33
		133–146	2	0.8		3.99	
		196–204	2	0.1	0.1	3.34	3.26
		205–218	2	0.3	−0.6	3.23	5.77
		219–252	3	0.6		3.76	
gi|15226791	PTAC12 (unknown protein)	106–121	2		0.6		2.66
At2g34640		127–142	2		0.6		4.41
		190–206	2	0.1		3.03	
		225–236	2	0.4		3.28	
		250–259	2		0.4		3.28
		269–283	2	−0.1		4.55	
		280–294	2	0.3		4.79	
		304–315	2		−0.4		2.70
		329–351	3	0.2		4.88	
		340–362	3	0.2		4.65	
gi|18398425	PTAC13 (KOW domain-containing transcription factor family protein)	65–70	1		−0.9		1.69
At3g09210		122–138	2	−0.5		3.05	
		174–185	2	0.6		2.51	
		198–209	2	−0.7		3.97	
		285–298	2	0.1		4.11	
gi|42566980	PTAC14 (SET domain-containing protein)	118–131	2	0.8		3.29	
At4g20130		224–230	1	0.6		1.70	
		250–260	2	0.1		2.92	
		337–350	2	−0.3		3.61	
		357–383	3	0.5		5.15	
		384–397	2	0.2		4.61	
		398–415	2	1.0		2.72	
gi|15239573	PTAC15 (mitochondrial transcription termination factor-related)	222–237	2	−0.2		4.15	
At5g54180		259–273	2	1.3		3.57	
		347–361	2	0.7		3.70	
gi|42565672	PTAC16 (expressed protein)	120–130	2	0.2		3.10	
At3g46780		149–164	2	0.3		3.13	
		237–248	2	0.8		2.87	

(Continued)

Table 1. (continued).

NCBI Acc. No./AGI Acc. No.[a]	Protein	Position[b]	Z[c]	ΔM[d]		x_{corr}[e]	
				Ara	*Sin*	*Ara*	*Sin*
		249–260	2	−1.9	−0.1	4.42	2.68
gi|15220146	PTAC17 (cobW	89–102	2		0.4		2.66
At1g80480	domain-containing protein)						
		208–218	2		−1.7		3.10
gi|15225202	PTAC18 (expressed protein)	75–93	2	0.7	−1.1	4.00	4.64
At2g32180		116–130	2	0.5		5.68	

Analysis of tandem MS (MS/MS) spectra is based on the *Arabidopsis* database (ftp://ftp.arabidopsis.org/home/tair/sequences/blast_datasets/).

[a] National Center for Biotechnology Information/Arabidopsis Genome Initiative accession numbers.

[b] Position of identified peptides within the database protein sequence.

[c] The charge state of the measured ion (z).

[d] The calculated deviation of the experimentally determined mass from the theoretical average mass of the peptide. Ara, *Arabidopsis*; Sin, *S. alba*.

[e] x_{corr} value calculated using the sequest algorithm.

the PEP transcription machinery. Based on run on transcription assays, pTAC2 is required for proper transcription of *psbA* by PEP but not for transcription for *atpB* and *clpP* by NEP. All three components might also be involved in posttranscriptional processes, such as RNA processing and/or mRNA stability.

RESULTS

Isolation of TAC from *Arabidopsis* and Mustard

In order to identify new components involved in plastid gene expression, we purified TACs from *Arabidopsis* and mustard. Several previously published purification protocols were combined to obtain highly purified TAC preparations (Rushlow and Hallick, 1982; Suck et al., 1996; Krause and Krupinska, 2000). After lyses of chloroplasts obtained by sucrose gradient centrifugation, soluble proteins were applied onto a Sepharose 4B column. Transcriptional active protein fractions were combined, and the TAC in these fractions was concentrated by ultracentrifugation. The precipitated complexes were dissolved and applied to a second column (either Sepharose 2B, Q Sepharose, or Heparin Sepharose CL-6B). Figure 1A demonstrates that the second gel filtration column causes a substantial enrichment of the specific transcriptional activity, similar to results reported previously for other species (Krause and Krupinska, 2000; data shown for Sepharose 2B). After phenol/chloroform extraction and tryptic digestion, these three preparations were directly used for mass spectrometry. Table 1 contains a list of 35 proteins that were identified with cross-correlation factor (x_{corr}) values >3.5, 2.5, and 1.5 for triple-, double-, and single-charged peptide ions in independent TAC preparations and with at least two independent peptides. Also present in our preparations were light-harvesting chlorophyll *a/b* binding proteins, D1, D2, and CP47 of photosystem II, α- and β-subunits of the ATP synthase, dihydrolipoamide *S*-acetyltransferase (At3g25860), and a putative ribulose-bisphosphate carboxylase activase (At1g73110), which were considered as contaminants.

Thirteen proteins identified in this preparation have also been identified in sRNAP preparations (Pfannschmidt et al., 2000;

Ogrzewalla et al., 2002; Loschelder et al., 2004; Suzuki et al., 2004). Seventeen of the polypeptides have been described earlier; however, only two of them were identified as components of the TAC. The other 18 proteins reported here have not yet been described. Computer analyses predicted plastid-directing transit sequences for 33 of the identified proteins. No clear information is available for pTAC9 (At4g20010) and pTAC13 (At3g09210).

Seventeen of the 35 polypeptides are involved in replication, transcription, translation, detoxification, protein modifications, or plastid metabolism. For the others, no function has been described. However, the domain structure of eight of them suggests that they might also be involved in replication, transcription, or translation. Besides the four subunits α, β, β′, and β″ of PEP, we identified Fe-dependent superoxide dismutases (SODs) and phosphofructokinases (PFKs). One of the identified SODs (SOD3, At5g22310) and one of the PFK-B-type enzymes (PFKB2, At3g54090) are also present in highly purified sRNAP preparations from mustard and tobacco (Pfannschmidt et al., 2000; Ogrzewalla et al., 2002; Loschelder et al., 2004; Suzuki et al., 2004). Among the known proteins, a putative DNA-polymerase A (At3g20540), two putative subunits of the DNA gyrase (At3g10690 and At3g10270), the elongation factor Tu (At4g20360), three ribosomal proteins (L12-A [At3g27830], S3 [ArthCp061], and L29 [At5g65220]), the UDP-*N*-acetylmuamoylalanyl-D-glutamate-2,6-diaminopimelate ligase (At1g63680), and a putative thioredoxin (At3g06730) have not yet been described as TAC components. The 18 new components were named plastid TAC proteins 1 to 18 (pTAC1-18). Based on the analyses of their domain structures, some of them contain either DNA or RNA binding domains, domains involved in protein–protein interactions, or epitopes described for other cellular functions (Table 2). However, database searches for four proteins did not reveal known functional domains.

Twenty-six of the 35 polypeptides were identified in TAC preparations from *Arabidopsis* and mustard (Tables 1 and 3), four proteins only in *Arabidopsis* (At3g20540, At5g23310, At2g46820, and At5g54180), and additional five only in mustard preparations (At3g27830, At5g65220, ArthCp061, At1g65260, and At1g80480). We isolated large amounts of TAC from mustard seedlings and

Table 2. Analysis of pTAC Domains

AGI Acc. No.[a]	Protein	cTP[b]	Domain[c]
At1g14410	PTAC1 (DNA binding protein p24-related)	+ (47)	ssDNA binding domain
At1g74850	PTAC2 (pentatricopeptide repeat-containing protein)	+ (66)	MutS PPR TPR
At3g04260	PTAC3 (SAP domain-containing protein)	+ (29)	SAP
At1g65260	PTAC4 (PspA/IM30 family protein)	+ (64)	PspA/IM30
At4g13670	PTAC5 (peptidoglycan binding domain-containing protein)	+ (40)	Peptidoglycan binding domain DnaJ
At1g21600	PTAC6 (expressed protein)	+ (59)	
At5g24314	PTAC7 (expressed protein)	+ (32)	
At2g46820	PTAC8 (expressed protein)	+ (45)	
At4g20010	PTAC9 (expressed protein)	−	DUF731 OB fold
At3g48500	PTAC10 (S1 domain- containing protein)	+ (40)	S1
At2g02740	PTAC11 (DNA binding protein p24-related)	+ (75)	ssDNA binding domain
At2g34640	PTAC12 (unknown protein)	+ (16)	
At3g09210	PTAC13 (KOW domain-containing transcription factor family protein)	−	KOW NGN
At4g20130	PTAC14 (SET domain-containing protein)	+ (62)	SET
At5g54180	PTAC15 (mitochondrial transcription termination factor-related)	+ (64)	mTERF
At3g46780	PTAC16 (expressed protein)	+ (19)	Nucleoside-diphosphate-sugar epimerases
At1g80480	PTAC17 (cobW domain-containing protein)	+ (68)	cobW
At2g32180	PTAC18 (expressed protein)	+ (32)	DUF861

[a] Arabidopsis Genome Initiative accession number.
[b] ChloroP prediction of the presence (+) or absence (−) of a transit sequence (cTP). The putative maturation site is given (Emanuelsson et al., 1999).
[c] Protein domains predicted by InterProScan (Apweiler et al., 2000) and BLAST (Altschul et al., 1997).

solubilized the proteins in Laemmli buffer after sonication. Twenty major bands could be visualized on a silver-stained gel, and they were identified by mass spectrometry (Figure 1B). Seventeen of these bands correspond to proteins also identified in unresolved TAC samples (Table 3). One additional protein not detected by the original mass spectrometry (MS) was found by analysis of the PAGE-derived protein bands (At2g05430). However, the size of protein bands resolved by PAGE does not always correspond to the predicted molecular masses of the polypeptides. This is not surprising considering that complete solubilization of the final TAC in the gel loading buffer could only be achieved by sonication. It appears that the proteins are tightly associated with each other or with nucleic acids. Some identified polypeptides contain RNA or DNA binding motifs, such as pentatricopeptide repeat motif (PPR), small MutS-related motif (SMR), SAP (for SAF-A/B, Acinus, and PIAS), S1, oligonucleotide/oligosaccharide binding (OB) fold, KOW (for Kyrpides, Ouzounis, and Woese), NGN, or mitochondrial transcription termination factor motif (mTERF) (Table 2). Therefore, it seems likely that the proteins identified in this study are components involved in plastid transcription/translation.

Identification and Characterization of Knockout Lines with Lesions in TAC Components

To further substantiate that pTACs are involved in plastid transcription, *Arabidopsis* knockout lines for pTAC2, -6, and

-12 were analyzed. *ptac2* (At1g74850) contains two nucleotide binding domains (PPR and SMR) and tetratricopeptide repeat (TPR) domains involved in protein–protein interaction. No obvious protein domains could be detected for *ptac6* (At1g21600) and *ptac12* (At2g34640). Mutations in homozygote knockout lines for these proteins are lethal when they were grown without exogenous carbon sources. DNA sequence analyses confirmed the positions of the T-DNA insertions provided by the Nottingham Arabidopsis Stock Centre (NASC) [At1g74850, 3rd exon after nucleotide 2571; At1g21600, 1st intron after the nucleotide 518; At2g34640, 8th intron after the nucleotide 2285 downstream of A(+1)TG codon]. RT-PCR with gene-specific primers uncovered that no more transcripts can be detected in *ptac2* (Figure 2). The small amounts of transcripts detected in *ptac6* and *ptac12* mutants might be due to the fact that the insertions are located in introns. However, the phenotype of the mutants clearly demonstrates that the residual transcript levels are too low to allow normal plastid development. A contamination of the RNA with genomic DNA can be excluded because the RT-PCR products do not contain intron sequences (Figure 2). Real-time PCR analyses with RNA from different organs of wild-type seedlings demonstrate that *ptac2*, *-6*, and *-12* transcripts are present in all tissues and that the mRNA levels are significantly reduced in roots (Figure 3). However, the presence of *ptac2*, *-6*, and *-12* transcripts in green and nongreen tissue suggests that the gene products are required in chloroplast and other types of plastids. It

Table 3. Identification of Bands from an SDS Polyacrylamide Gel with Mustard TAC Proteins

Band	MM (kD)	Protein	Position[a]	Z[b]	ΔM[c]	x_{corr}[d]	AGI Acc. No.[e]
1	19–21	Thioredoxin, putative	79–90	2	−0.2	4.35	At3g06730
			80–90	2	−0.5	4.04	
			132–142	2	−0.3	3.83	
			148–161	2	−0.1	4.16	
		Ribosomal protein L29p	97–103	1	1.1	1.68	At5g65220
2	22–23	Hypothetical protein	140–156	2	−1.2	2.50	At2g05430
3	24–25	Ribosomal protein S3	92–101	2	−0.3	3.19	ArthCp061
			184–192	1	0.4	1.71	
4	26–28	?					
5	30–32	Hypothetical protein	140–156	2	−0.4	2.51	At2g05430
6	33–35	PTAC4 (PspA/IM30 family protein)	146–152	2	0.2	1.54	At1g65260
			223–241	2	−0.4	3.03	
			246–267	2	1.4	2.70	
			268–284	2	0.9	3.14	
		PTAC6 (expressed protein)	272–279	2	−1.1	2.59	At1g21600
7	36–38	?					
8	39–40	PTAC1 (DNA binding protein p24-related)	81–89	2	−0.7	2.55	At1g14410
			181–199	2	1.2	3.78	
			248–263	2	−1.5	2.93	
		PTAC11 (DNA binding protein p24-related)	196–204	2	−0.4	2.82	At2g02740
9	42–44	PTAC14 (SET)	90–96	1	0.8	1.58	At4g20130
		PTAC11 (DNA binding protein p24-related)	85–93	2	−0.7	2.55	At2g02740
			96–103	1	0.4	1.53	
			104–116	2	1.2	2.56	
			120–134	2	−1.1	4.15	
			196–204	2	−0.4	2.63	
			253–259	1	0.1	1.91	
			260–268	2	0.7	3.11	
10	54–55	Iron superoxide dismutase (FE-SOD1)	253–262	2	−0.4	2.92	At5g51100
		pfkB-type carbohydrate kinase family protein (PFKB1)	578–597	2	−0.2	2.70	At1g69200
		PTAC12 (unknown protein)	127–142	2	0.1	2.53	At2g34640
			249–259	3	−0.7	3.51	
11	60–62	RNA polymerase β″-chain (RpoC2)	1083–1091	2	−0.7	3.22	ArthCp012
		PTAC9 (expressed protein)	121–130	2	−0.1	3.20	At4g20010
			288–299	2	−0.1	3.12	
12	70–72	PTAC6 (expressed protein)	149–161	2	−0.5	3.02	At1g21600
			189–208	2	−0.2	3.36	
			209–213	1	0.0	1.62	
			273–279	1	0.3	1.54	
			303–307	1	0.6	1.55	
		pfkB-type carbohydrate kinase family protein (PFKB2)	146–160	2	−0.6	3.20	At3g54090
			165–170	1	0.2	1.57	
13	78–80	RNA polymerase β′-chain (RpoC1)	327–341	2	−0.7	3.28	ArthCp013
			461–474	2	−1.4	4.02	
			595–605	2	−1.0	3.01	
		PTAC6 (expressed protein)	149–161	2	−0.7	2.69	At1g21600
		Hypothetical protein	140–145	2	0.0	2.60	At2g05430
		PTAC4 (PspA/IM30 family protein)	99–113	2	−0.2	2.59	At1g65260
			246–267	2	0.4	4.76	
			268–284	2	1.4	3.62	
		Mur ligase family protein	570–580	2	0.7	2.66	At1g63680
14	82–84	PTAC10 (S1 domain-containing protein)	593–606	2	0.0	3.52	At3g48500
			609–622	2	−1.0	2.52	
15	85–87	PTAC5 (peptidoglycan binding domain-containing protein)	80–92	2	−1.0	3.26	At4g13670
16	88–91	PTAC5 (peptidoglycan binding domain-containing protein)	80–92	2	−0.2	3.56	At4g13670
17	95–100	PTAC11 (DNA binding protein p24-related)	104–116	2	−0.9	3.68	At2g02740

(Continued)

Table 3. (continued).

Band	MM (kD)	Protein	Position[a]	Z[b]	ΔM[c]	x_{corr}[d]	AGI Acc. No.[e]
			120–134	2	−0.1	3.48	
			196–204	2	−1.3	2.55	
18	135–145	PTAC10 (S1 domain-containing protein)	41–46	2	−0.3	3.18	At3g48500
			72–76	1	0.1	1.53	
			95–114	2	0.7	3.47	
			172–177	1	0.2	1.61	
			383–403	2	0.2	2.84	
			484–489	1	0.2	1.62	
19	150–160	PTAC3 (SAP domain-containing protein)	496–515	2	−0.5	3.92	At3g04260
			703–713	2	−0.3	2.85	
			618–631	2	0.2	4.22	
		RNA polymerase β″-chain (RpoC2)	1083–1091	2	0.0	2.63	ArthCp012
			1144–1151	2	−0.5	2.91	
			1206–1214	2	1.1	2.53	
20	165–175	RNA polymerase β-chain (RpoB)	646–977	2	−0.2	3.29	ArthCp014
		RNA polymerase β″-chain (RpoC2)	138–150	2	−0.2	3.78	ArthCp012
			266–276	2	−0.2	2.53	
			511–525	2	−0.1	3.09	
			1144–1151	2	−0.6	2.74	

Analysis of MS/MS spectra is based on the *Arabidopsis* database (ftp.arabidopsis.org/home/tair/sequences/blast_datasets/). MM, molecular mass in kilodaltons.

[a] Position of identified peptides within the database protein sequence.

[b] The charge state of the measured ion (z).

[c] The calculated deviation of the experimentally determined mass from the theoretical average mass of the peptide.

[d] x_{corr} value calculated by using the sequest algorithm.

[e] NCBI/AGI accession numbers.

remains to be determined whether the amounts of these proteins correlate with the number of plastids or nucleoids per cell.

The homozygote seedlings develop white cotyledons, fail to accumulate chlorophyll even under low light intensities, and do not produce primary leaves. On sucrose medium, the mutants reach the rosette stage, but they are much smaller and grow slower than the wild type (Figure 4). While *ptac2* develops yellow cotyledons and greenish primary leaves on sucrose medium, the other two mutants stay more yellowish. By contrast, dark-grown *ptac* plants show the phenotype of the etiolated wild type. A detailed analysis of pigments from low-light-grown *ptac* plants revealed that chlorophylls and carotenoids accumulate in the mutants, although the overall amounts are quite low. The decrease of total chlorophyll (∼70% in *ptac2*, ∼99% in *ptac6*, and ∼95% in *ptac12* plants) was accompanied by a noticeable decrease in the chlorophyll *a:b* ratio in *ptac2* and *-12* and increase in *ptac6* plants (Table 4). These changes might be due to an increase in the photosystem II light-harvesting system and/or a decrease in the photosystem I:II ratio in case of *ptac2* and *-12* and the opposite for *ptac6* plants, respectively. Furthermore, we observed a significant increase in the carotenoid: chlorophyll as well as in the xanthophyll:chlorophyll ratio (Table 4) in mutant seedlings. Interestingly, the antheraxantin level is relatively high and the zeaxanthin level below detectability. Both xanthophyll pigments are not detectable in the wild type, which is known to be the case for plants grown under moderate conditions (Demmig-Adams and Adams, 2002). Fluorescence quenching analysis indicates effects on photochemical efficiency

in the mutant lines. As shown in Table 4, the maximum quantum yield (Fv/Fm) and photochemical quenching [(Fm′ − Ft)/Fm′] are significantly lower than those of the wild type. The reduced ratio of variable-to-maximum fluorescence (Fv/Fm) indicates smaller
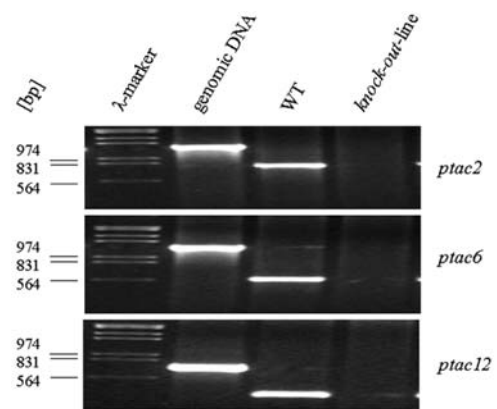

Figure 2. Mutant Analyses.

The knockout lines *ptac2*, *-6*, and *-12*, which were determined to be homozygotes by PCR, fail to accumulate normal amounts of messages from the inactivated genes. Total RNA was isolated from wild-type and knockout seedlings and used for RT-PCR with gene-specific primers. *ptac2* (34 cycles), *ptac6* (30 cycles), and *ptac12* (45 cycles). DNA: PCR with genomic DNA from wild-type seedlings (23 cycles). Size markers in kilobases are at left.
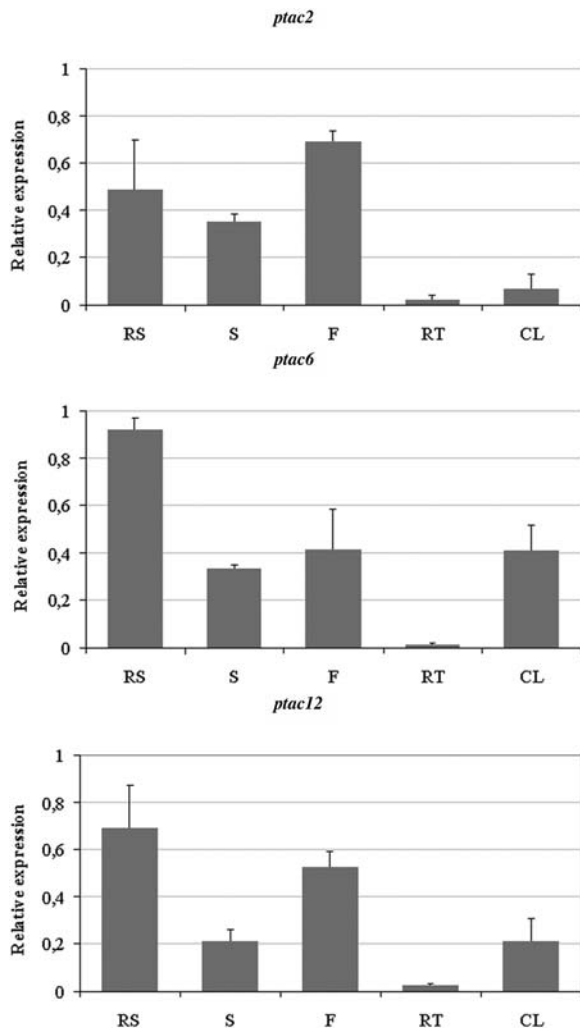
Figure 3. Tissue-Specific Expression of *ptac2*, *-6*, and *-12*.

An equal amount of cDNA from the cotyledons (set as 1.0), rosette leaves (RS), stems (S), flowers (F), roots (RT), and cauline leaves (CL) from *Arabidopsis* was used for real-time PCR with gene-specific primers for the actin gene (Robinson et al., 1999), *ptac2*, *-6*, and *-12*. Fold induction values of genes were calculated with the $\Delta\Delta$CP equation of Pfaffl (2001) and related to the mRNA level of the genes in cotyledons, which was defined as 1.0. This value is not shown in the graph. The data shown here were obtained from three independent experiments, and the error bars represent standard deviation.

photosystem II antennae and/or fewer functional photosystem II centers (Meurer et al., 1998). In accordance with this observation, *ptac2* reveals higher values of nonphotochemical quenching (NPQ; Krause and Weis, 1991). In case of *ptac6* and *-12*, the NPQ values might be caused by the reduced chlorophyll contents.

Analysis of the plastid structure in the mutants showed that the organelle development is severely impaired (Figure 5). Compared with the wild type, grana structures in *ptac2* plants are unequally expanded. Grana-interlacing stroma thylakoids are completely missing (Figure 5B). Chloroplasts of *ptac6* and *ptac12*

plants do not contain grana thylakoids. They are replaced by oval-shaped vesicles (Figures 5C and 5D). Surprisingly, an accumulation of starch is only observed in the old leaves of *ptac6* and *ptac12* mutants. Frequently a multiplicity of plastoglobuli is found in close proximity to the above-mentioned vesicles (Figures 5B and 5C). Both plastid- and nuclear-encoded soluble polypeptides and polypeptides associated with the thylakoid membrane are either absent or strongly reduced in the mutants (Figure 6). Since plastid-encoded polypeptides, such as the large subunit of ribulose-1,5-bis-phosphate carboxylase/oxygenase, subunit IV of cytochrome b_6/f complex, and $CF_1\varepsilon$, are still detectable in all three mutants, the mutations do not affect general processes in plastid transcription and/or translation.

Macroarray analyses demonstrated that all plastid-encoded genes are expressed in the mutants. In most cases, these data confirmed the results obtained by RNA gel blot analyses. Differences in the mRNA results might be caused by radiolabeled antisense RNA, which also hybridized to the probes (Krause et al., 2000; Legen et al., 2002). However, compared with the wild type, we observed remarkable alterations (Figure 7). The transcript levels for components of the two photosystems and for the cytochrome b_6/f complex are significantly reduced. For instance, the *psbA* mRNA level (for the D1 protein) in *ptac2* and *ptac12* and the *psbA*, *psbC*, and *psbE* mRNA levels (for CP43 and cytochrome b_{559}/2) in *ptac6* plants are reduced by 80 and 50%, respectively. In all three mutants, *petB* (for a subunit of the cytochrom b_6/f complex) and *rbcL* (for the large subunit of ribulose-1,5-bis-phosphate carboxylase/oxygenase) transcripts accumulate to <50%. These mRNAs are probably transcribed from genes with PEP promoters. By contrast, *rps*, *rpl* (for ribosomal proteins), *ndh* (for subunits of the NADH dehydrogenase), *atp* (for subunits of the ATP synthase), *rpo* (for subunits of the RNA polymerase), and *ycf* (for hypothetical chloroplast open

Figure 4. Phenotype of *ptac2*, *-6*, and *-12* Mutant Plants.

Ptac2, *-6*, and *-12* and wild-type seedlings after 12 **(A)** and 18 **(B)** d grown on Murashige and Skoog medium under long-day conditions.

**Table 4.** Pigment Analysis and Fluorescence Measurements of Wild-Type and Mutant Lines

	Pigment Composition			Chlorophyll Fluorescence Measurements		
Line	Chlorophyll a/b (mol/mol)	Carotenoids/Chlorophyll (mol/mol)	VAZ/Chlorophyll (mmol/mol)	Fv/Fm	(Fm′ − Ft)/Fm′	NPQ
Wild type	3.2 ± 0.034	0.25 ± 0.008	40.7 ± 1.4	0.854 ± 0.012	0.719 ± 0.037	0.456 ± 0.030
tac2	2.8 ± 0.106	0.35 ± 0.012	99.1 ± 4.8	0.497 ± 0.055	0.365 ± 0.039	0.890 ± 0.226
tac6	4.4 ± 0.286	1.48 ± 0.071	467.9 ± 18.0	0.424 ± 0.089	0.371 ± 0.073	0.324 ± 0.058
tac12	2.8 ± 0.057	0.60 ± 0.042	216.7 ± 13.5	0.546 ± 0.013	0.395 ± 0.022	0.399 ± 0.044

Pigment data are the average of three independent samples. Flourescence quenching analysis is averaged from nine plants. VAZ is the xanthophyll pool size (violaxanthin + antheraxanthin + zeaxanthin).

reading frames) genes are expressed at higher levels in all three mutants. These messages are transcribed from genes that may contain NEP promoter elements, either alone or in combination with PEP promoter elements. The expression pattern of the plastid genes in the mutants is identical to that described for Δ*rpo* mutants and mutants that do not accumulate PEP. These mutants also contain reduced transcript levels for photosynthesis proteins, while *ndh*, *atp*, and *rpo* genes are expressed at higher levels (Hess et al., 1993; Allison et al., 1996; Hajdukiewicz et al., 1997; Silhavy and Maliga, 1998; De Santis-Maciossek et al., 1999; Krause et al., 2000; Legen et al., 2002). However, for some plastid genes (e.g., for *clpP*), the expression level in the wild type was not significantly different from the background. Finally, the reduced *psbA* mRNA level in *ptac2* plants is caused by a reduced rate of *psbA* transcription as shown by run-on transcription assays, while transcription of *atpB* and *clpP* appear to be not affected in the mutant (Figure 8). We could not obtain enough chloroplasts from the homozygote mutants to unambiguously confirm this for the other genes and mutants.

To further substantiate the findings derived by macroarray analyses, representative genes were chosen for RNA gel blot analyses (Figure 9). Figure 9A shows genes (*psaAB*, *psaC*, *psaJ*, *psbA*, *rbcL*, and *rps14*) that are downregulated in the mutants, Figures 9B and 9D shows genes (*atpB*, *clpP*, and the nuclear-encoded genes *psaH*, *psaE*, and *psbO*) that do not respond significantly to the mutations, and Figure 9C shows genes (*accD*, *atpA*, *ndhF*, *ndhB*, and *ycf3*) that are upregulated in the mutants. Genes shown in Figure 9A contain only PEP promoter sequences, and their expression is also downregulated in Δ*rpo* mutants and other mutants impaired in PEP function (Hess et al., 1993; Allison et al., 1996; Hajdukiewicz et al., 1997; Silhavy and Maliga, 1998; De Santis-Maciossek et al., 1999; Krause et al., 2000; Legen et al., 2002). By contrast, the Figures 9B and 9C show genes that contain NEP promoter elements either alone or in combination with PEP promoter elements. Again, these genes exhibit the same expression behavior in Δ*rpo* mutants and other mutants impaired in PEP function (Hess et al., 1993; Allison et al., 1996; Hajdukiewicz et al., 1997; Silhavy and Maliga, 1998; De Santis-Maciossek et al., 1999; Krause et al., 2000; Legen et al., 2002). Furthermore, we observed in all mutants defects in mRNA processing, since larger transcripts accumulate for *accD*, *atpB*, *clpP*, *ndhB*, *ndhF*, *psaAB*, *rbcL*, *rps14*, and *ycf3*. This is most obvious for the polycistronic transcript *ycf3/psaA/psaB/rps14*. Besides mRNAs with 3.2 and 5.2 kb, additional messages with 5.8 and 7.3 kb hybridize to the *psaAB* probe in the mutants. They

represent unprocessed transcripts and include sequences for *ycf3*, as shown by the hybridization with the *ycf3*-specific probe (Figure 9C; Summer et al., 2000; Legen et al., 2002). Again, the very same lesions in the processing patterns were observed for Δ*rpo* mutants and other PEP mutants. Taken together, these data suggest that the expression of genes encoding the three novel TAC proteins is required for proper function of PEP transcription machinery. Since messages for all genes studied are present in all three mutants and since at least some of them are also properly processed, the mutations do not completely inhibit crucial steps in plastid transcription or translation. pTAC2 and pTAC6 are also present in sRNAP preparations (Suzuki et al.,
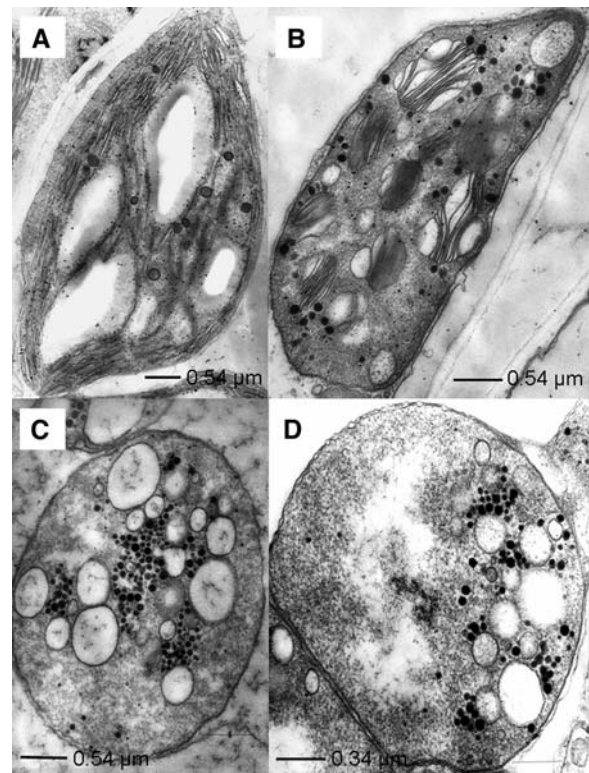
Figure 5. Ultrastructure of Plastids from Wild-Type and Mutant Seedlings.

The wild type **(A)**, *ptac2* **(B)**, *ptac6* **(C)**, and *ptac12* **(D)**.
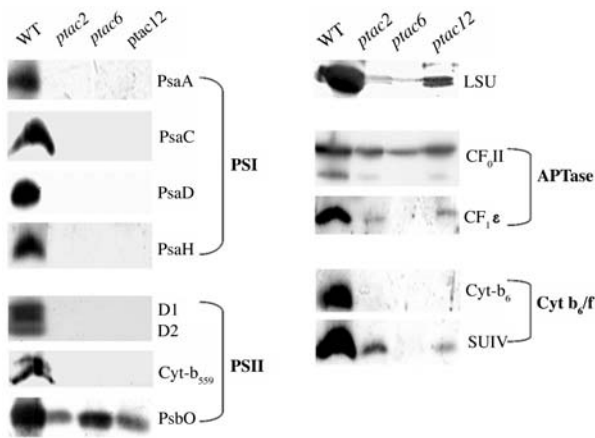
Figure 6. Immunoblot Analyses of Plastid Proteins.

Fifteen micrograms of plastid proteins of wild-type and mutant (*ptac2*, *-6*, and *-12*) seedlings were separated on polyacrylamide gels containing SDS. The immunological detection of the proteins occurred with antibodies against the subunits A, C, D, and H of photosystem I (PSI), against D1/2, cytochrome b_{559} and PsbO of photosystem II (PSII), against CFoII and $CF_1\varepsilon$ of the ATP synthase, against cytochrome b_6 and the subunit IV of the cytochrome *b_6/f* complex, and against the large subunit of ribulose-1,5-bis-phosphate carboxylase/oxygenase (LSU).

2004), suggesting that they are preferentially involved in transcription rather than translation.

To analyze the effect of the pTAC-2, -6, and -12 mutations on PEP and NEP promoter activity in leaf tissue, we determined transcript levels by primer extension analyses mapping transcript 5′-ends for *clpP* and *atpB*, two representative plastid genes with NEP and PEP promoter elements (Figure 10). In these studies, we also included the pale-yellow-green (*pyg*) mutant 8 (lane 10; J. Stöckel and R. Oelmüller, unpublished data) because it exhibits a very similar phenotype and growth behavior as the *ptac* mutants. Since signals at the promoter initiation site are dependent on the mRNA level, we included into our investigations only such genes whose mRNA levels are not affected by the mutations. We did not observe any significant difference in the signal intensities at the NEP promoter site P-57 of *clpP* (panel *clpP*; Sriraman et al., 1998). This example indicates that the NEP promoter usage is not altered in the *ptac* and *pyg* mutants. By contrast, the signal at the P-515/-520 PEP side of *atpB* is dramatically downregulated in *ptac2* and *ptac12* mutants (panel *atpB*, lanes 6 and 8) and below detectability in *ptac6* plants (lane 7). Sequence alignments of *atpB* promoter sequences from different species indicate that the conserved regions represent PEP (-35/-10) elements (data not shown). Since the primer extension signal at this PEP site is nearly equal in the wild type and in the *pyg8* mutant (Figure 10, lanes 9 and 10), it appears that the PEP promoter usage is specifically affected in the *ptac* mutants.

The expression of *ptac2*, *-6*, and *-12* in organs with different types of plastids (Figure 3) suggests that the gene products are required for general processes of the PEP activity and not restricted to photosynthetically active plastids. To test this further and to exclude the possibility that the phenotypes of the mutants grown in low light (see Methods) are caused by photooxidative damage due to light stress, we repeated the RNA gel blot and primer extension analyses with etiolated material. Segregating populations were germinated in low light for 3 d to identify the homozygote seedlings. They were then transferred to complete darkness for an additional 18 d before harvest of the newly emerged etiolated leaves. RNA gel blot analyses for representative genes of the three classes described above (Figure 9) clearly indicate that the observed differences in the transcript levels in the mutants are not light dependent (Figure 9E). Furthermore, primer extension analysis for *atpB* also gave comparable results as obtained for seedlings grown in low light (data not shown; Figure 10). Finally, as described for seedlings grown in low light, the *atpB* transcript levels in etiolated material are similar or even higher in *ptac2* and *-12* plants (Figure 9E), although the primer extension signals at the PEP sites were downregulated (data not shown). This clearly indicates that *ptac2*, *-6*, and *-12* function is not related to thylakoid biogenesis, photosynthesis, or photooxidative stress.

DISCUSSION

We hypothesized that nuclear-encoded components required for transcription and translation in plastids might be associated with the TAC. TAC preparations from various organisms were analyzed on SDS gels, and in this way, at least 40 polypeptides associated with TAC have been detected. However, only the α- and β-subunits of the PEP (Suck et al., 1996; Krause and Krupinska, 2000), a homolog of the nuclear transcription elongation factor TFIIS (da Costa e Silva et al., 2004), and few plastid DNA–bound proteins, including PEND (Sato et al., 1993), sulfite reductase (Cannon et al., 1999; Chi-Ham et al., 2002; Sekine et al., 2002), CND41 (Murakami et al., 2000), and MFP1 (Jeong et al., 2003), have been identified until now. We used different gel filtration and affinity chromatography purification steps for the isolation of TACs from mustard and *Arabidopsis.*

The available sequence information allowed us to identify the *Arabidopsis* TAC components with high fidelity and to analyze their role in knockout lines. Furthermore, this allowed us to compare the TAC composition of two related organisms. Using the above-mentioned criteria (at least two independent peptides in independent preparations), we identified 35 polypeptides in our TAC preparations, 18 of these components have not yet been described so far (cf. also below). We could demonstrate that three of them influence plastid transcription, RNA accumulation, and processing and therefore are essential for plastid gene expression.

Twenty-five polypeptides could be identified in TAC preparations from *Arabidopsis* and mustard (Tables 1 and 3). Four additional proteins (At3g20540, At5g23310, At2g46820, and At5g54180) were only detected in *Arabidopsis* TAC preparations. Only five polypeptides were identified in mustard but not in the *Arabidopsis* TAC (At3g27830, At5g65220, ArthCp061, At1g65260, and At1g80480). These differences might be caused by the different developmental stages of the plastids, by the different abundance of individual proteins in the two species, or by the fact that the identification of mustard proteins with *Arabidopsis* databases is not possible in all instances. Based on homology searches, the
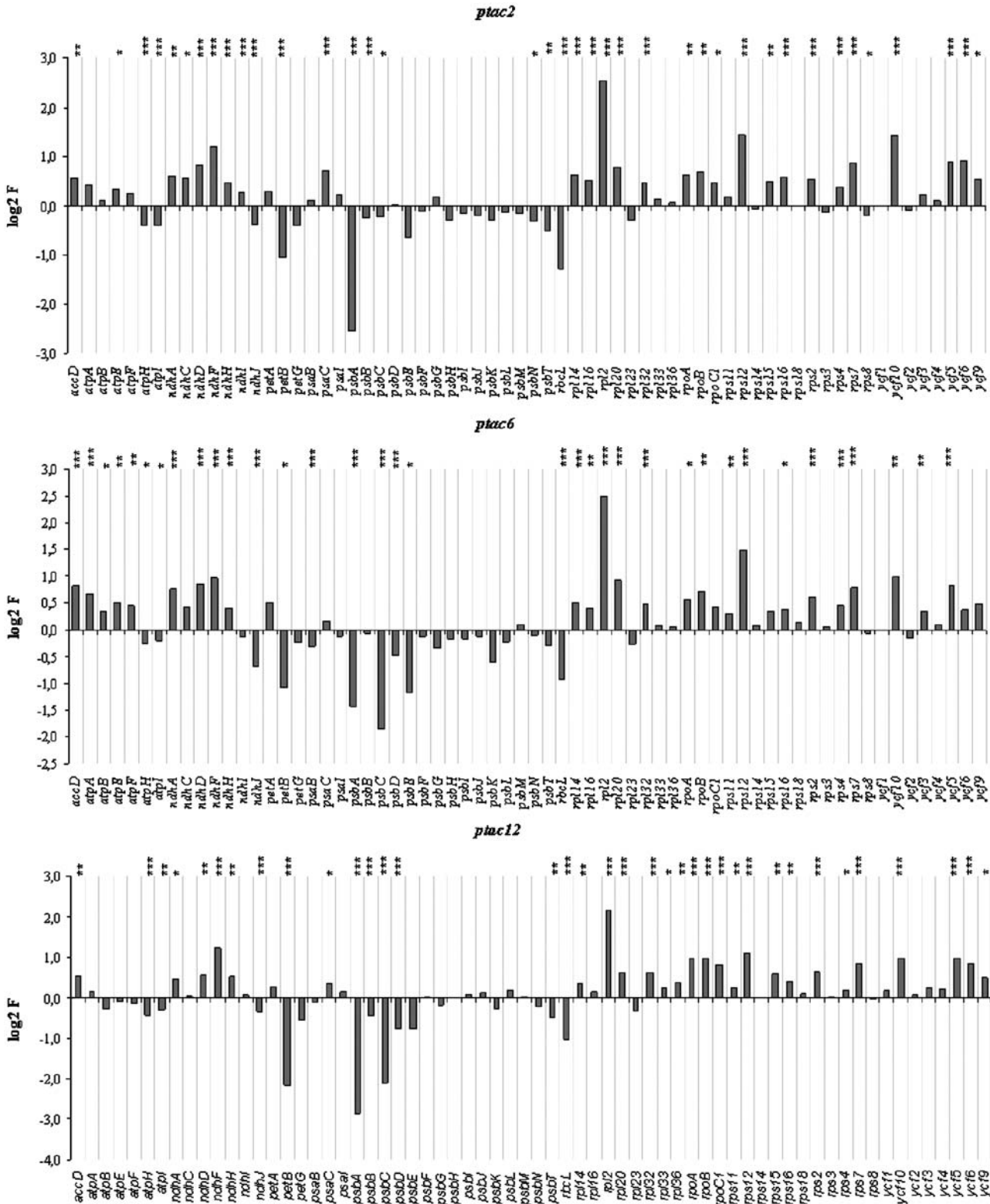
Figure 7. Changes in Transcript Abundance of Plastome-Encoded Genes.

A macroarray representing all protein-coding genes of the plastome was hybridized with probes synthesized from the mutants (*ptac2*, *ptac6*, and *ptac12*) and wild type. The diagram shows the $\log_2$ induction factor ($\log_2$ IF). IF was calculated from the ratio of the mutant and wild-type signal intensities. $\log_2$ IF is given where 3.32 corresponds to a 10-fold upregulation and -3.32 to a 10-fold downregulation. *** Indicates $P < 0.05$, ** indicates $0.05 < P < 0.10$, and * indicates $0.10 < P < 0.20$.
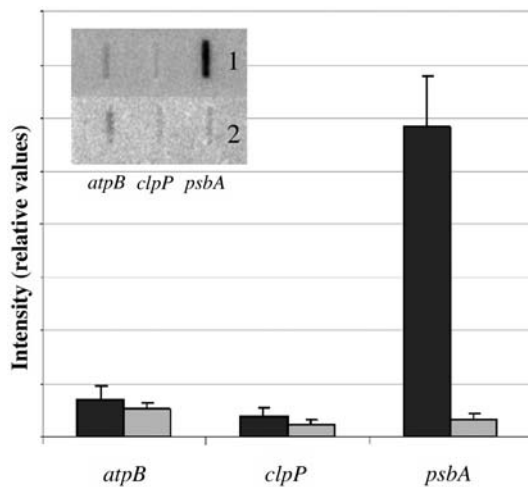
Figure 8. Analyses of Transcription Rates.

For run-on transcription assays of *atpB*, *clpP*, and *psbA*, 2×10^7 chloroplasts were used from wild-type (inset 1) and *ptac2* (inset 2) plants. The quantification of signal intensities occurred with a Storm Phosphor-Imager. The signals were normalized to total signal intensity within mutants and the wild type, respectively. Error bars represent corresponding standard deviation.

TAC contains polypeptides involved in replication, transcription, translation, detoxification, protein modification, and plastid metabolism. Eleven identified proteins are DNA or RNA binding proteins or complexes (α-, β-, β'-, and β''-subunits of PEP, a putative DNA polymerase A, two putative subunits of the DNA gyrase, the elongation factor EF-Tu, and three ribosomal proteins, S3, L12-A, and L26). Eight additional proteins contain DNA/RNA binding domains, such as the PPR, SMR, SAP, OB fold, S1, KOW, NGN, mTERF, or single-stranded DNA (ssDNA) binding motifs (Table 2). These motifs are found in proteins involved in chromatin organization, DNA repair, transcription, RNA processing, or translation (Boni et al., 1991; Kyrpides et al., 1996; Fernandez-Silva et al., 1997; Draper and Reynaldo, 1999; Moreira and Philippe, 1999; Aravind and Koonin, 2000; Lurin et al., 2004). Furthermore, pTAC1 and pTAC11 exhibit striking similarities to p24 proteins, which are members of the Whirly proteins of nuclear transcription factors (Desveaux et al., 2002, 2004). All Whirly proteins have target sequences for organelles (Krause et al., 2005); thus, they might be dually targeted to the nucleus and the plastid. The exact functions of the pTAC proteins remain to be determined; however, the striking similarities of the observed phenotypes of the knockout lines for three of these proteins with those of Δrpo mutants and other mutants impaired in PEP function suggests that they are also involved in plastid gene expression. Like Δrpo plants, *ptac2*, *-6*, and *-12* mutants are defective in plastid gene transcription as well as proper mRNA processing and/or stability, suggesting that they belong to a complex that is involved in different steps of plastid gene expression. This is particularly interesting for pTAC6 and -12, two plastid-localized proteins for which no domains or functions could be predicted. Only the presence of these proteins in our TAC preparations in combination with the observed phenotype

of the knockout lines allows us to predict a role of these proteins in plastid gene expression.

In *Escherichia coli* and bacteriophage λ, different proteins, including subunits of the ribosomes, are components of the transcription and translation machinery, at least during some stages of the cell cycle (Zellars and Squires, 1999). Some RNAP subunits play an important role during transcription initiation, antitermination, elongation, and termination (Squires and Zaporojets, 2000). Moreover, many ribosomal proteins participate in the transcription of their own genes or of rRNA genes (Zengel et al., 1980; Squires and Zaporojets, 2000). Oleskina et al. (1999) also identified ribosomal proteins that are associated with plastid DNA. Studies on phage Q replication demonstrated that S1 and the elongation factors EF-TU and EF-TS are also subunits of the β-RNA replicase (Brown and Gold, 1996). Likewise, EF-Tu, S3, L12, and L29 could have a dual function in plastid gene expression in that they coordinate replication, transcription, and translation. Furthermore, pTAC15 contains a KOW domain, which is characteristic for members of the NusG protein family (Kyrpides et al., 1996). NusG is an essential factor for coupled transcription/translation in *E. coli* and bacteriophage λ (Zellars and Squires, 1999).

While a putative DNA polymerase (Kimura et al., 2002) and two subunits of the topoisomerase II (Reece and Maxwell, 1991; Cho et al., 2004) are primarily involved in replication and the four plastid-encoded subunits α, β, β', and β'' of PEP in transcription in the TAC, the exact role of the other components identified in this fraction is less clear. A Fe-SOD has also been detected in the PEP-A complex of a soluble plastid fraction from mustard (Pfannschmidt et al., 2000; Ogrzewalla et al., 2002; Loschelder et al., 2004), together with putative kinases, which we did not find in our preparations. The absence of the cpk2 kinase can be explained by the loose association with the sRNAP (Baginsky et al., 1997). Our data indicate that at least two Fe-SODs are present in our TAC preparations. They might function as protective agents against reactive oxygen species (Pfannschmidt et al., 2000). Hydrogen peroxides, for instance, can stimulate transcription of plastid *ndh* genes under photooxidative stress (Casano et al., 2001). We also identified two PFKs in the TAC, one of them was also found in sRNAP preparations (Suzuki et al., 2004). PFK might couple the expression of photosynthesis genes to sucrose signals in the plant cell (Oswald et al., 2001). Finally, thioredoxin, which was also identified in our preparations, regulates key enzymes in the plastids via redox signals (Schürmann and Jacquot, 2000). In *Rhodobacter sphaeroides*, expression of genes from the *puf* operon is controlled by thioredoxin (Pasternak et al., 1999). Furthermore, redox signals via thioredoxin are able to influence gene expression by affecting gyrase activity (Li et al., 2004). Thus, the association of these components to the TAC might ensure its regulation in response to various signals.

We could not identify the TAC component ET1, which was recently detected immunologically in maize (*Zea mays*) (da Costa e Silva et al., 2004). However, it cannot be excluded that this protein is present in the TAC fraction. It is conceivable that ET1 was not detected by MS because of simultaneous elution of other abundant peptide ions. Presumably, it is also the case with the nuclear-encoded RNA polymerase RpoTp (*RpoT;3*; At2g24120), which we could only identify with scores slightly below our
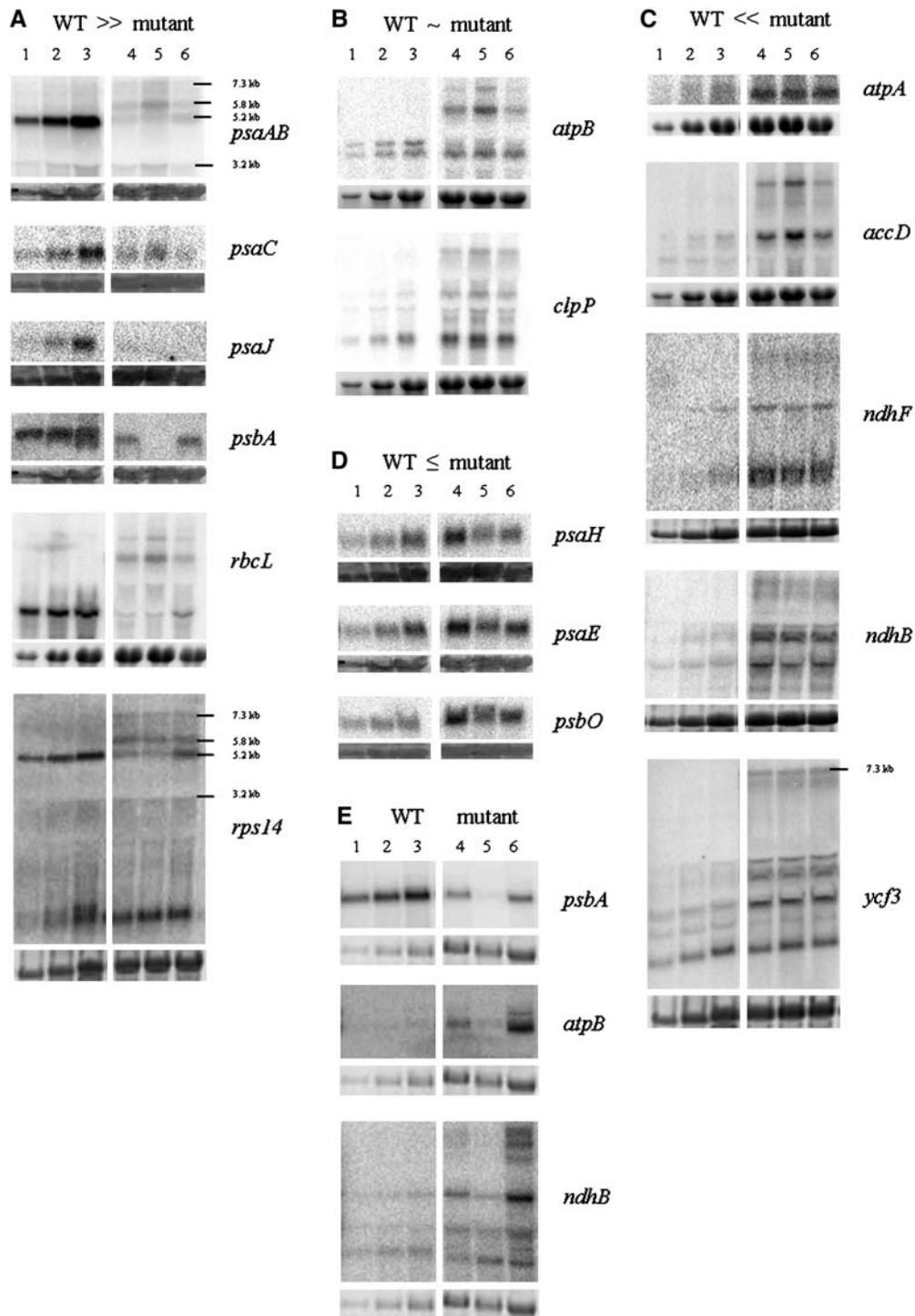
Figure 9. Transcript Accumulation.

RNA gel blot analyses for plastid- and nuclear-encoded genes were performed with RNA from wild-type (lanes 1 to 3) and mutant (lane 4, *ptac2*; lane 5, *ptac6*; lane 6, *ptac12*) seedlings. RNA loaded per lane is as follows: 3.25 μg (lane 1), 7.5 μg (lane 2), and 15 μg RNA (lanes 3 to 6). The gene probes are indicated. The 18S rRNA accumulation is shown in the ethidium bromide–stained gels below each plot to confirm equal loading. Bars mark the position of cotranscripts.

(A) and **(C)** The transcript levels are reduced (enhanced) in the mutants.

(B) The amount of transcripts is similar in the wild type and mutants.

(D) RNA gel blot analyses of nuclear-encoded genes.

(E) RNA gel blot analyses of 18-d-old dark-grown material.
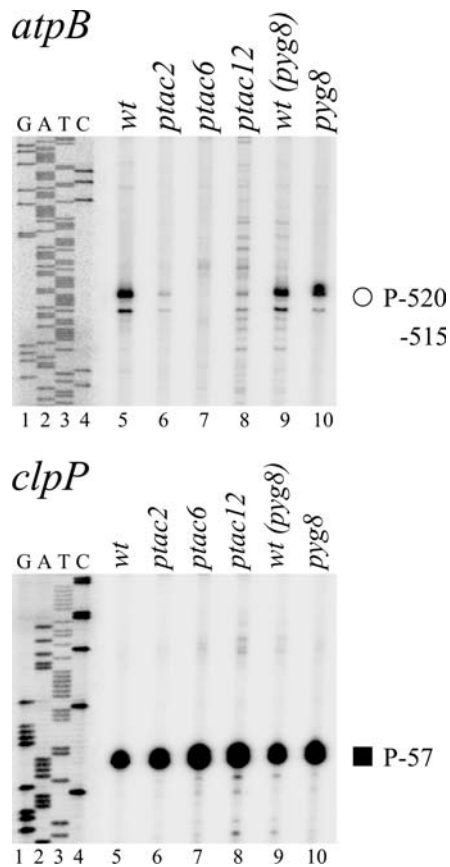
Figure 10. Primer Extension Analyses of *ptac2*, *ptac6*, *ptac12*, and the Wild Type.

In *ptac* knockout plants (lanes 6 to 8), transcript accumulation from the PEP *atpB*-515/520 promoter is negatively affected compared with the wild type (lane 5) but not from the type-II *clpP*-57 NEP promoter. Primer extension data are shown for the *atpB* and *clpP* genes. Mapped PEP (open circle) and NEP type-II (closed square) promoters are identified by their distance between the transcription initiation site and the translation initiation codon in nucleotides (K. Kühn, D. Kaden, and K. Liere, unpublished data; Sriraman et al., 1998). For reference, the same end-labeled primer was used to generate a DNA sequence ladder (lanes 1 to 4). The *pyg8* mutant (lane 10; J. Stöckel and R. Oelmüller, unpublished data) and the corresponding wild type [wt(*pyg8*); lane 9] were used as independent controls for transcriptional activity.

standard criteria (x_{corr}: 2.47 for the double-charged peptide ion $_{294}$[KNNAGDSQEELK]$_{305}$ and 1.59 for the single-charged peptide ion $_{149}$[IERKDIDK]$_{156}$). In future experiments, multdimensional chromatography (e.g., strong cation exchange coupled with reversed-phase liquid chromatography) would probably enable the identification of more peptides by MS, especially low abundant ones. As mentioned above, Table 1 contains only those proteins that were identified by at least two independent peptides in independent preparations. At least 40 other candidate proteins that do not fulfill this criterion were also identified in our preparation, and four of them have been described before as putative candidates of the TAC. This includes PEND (Sato et al., 1993), sulfite reductase (Cannon et al., 1999; Chi-Ham et al.,

2002; Sekine et al., 2002), CND41 (Murakami et al., 2000), and MFP1 (Jeong et al., 2003). Some of them are clearly contamination of other plastid multiprotein complexes, such as the small subunit of ribulose bisphosphate carboxylase, PsbS (subunit S of the photosystem II), the α-subunit of carboxyltransferase, and a putative ferritin subunit (At3g11050). Thus, additional work is required to clearly demonstrate which proteins are tightly associated with TAC.

The role of the new components identified in our studies is more enigmatic. *Arabidopsis* knockout lines for three of these components were analyzed in this study. These components have been chosen because bioinformatic analysis would not allow any prediction of their association with TAC. The knockout lines have severe lesions in plastid transcription and RNA metabolism that lead to almost identical phenotypes reported for Δrpo mutants and mutants that do not accumulate PEP (Hess et al., 1993; Allison et al., 1996; Hajdukiewicz et al., 1997; Silhavy and Maliga, 1998; De Santis-Maciossek et al., 1999; Krause et al., 2000; Legen et al., 2002). While transcripts for all plastid-encoded genes can be detected in the mutants, their expression profiles differ. For some genes, <10% of the wild-type transcript level can be detected. Interestingly, transcription of such genes is only driven from PEP promoters. Expression of genes with NEP promoters is either not altered or upregulated. Similar to the expression profiles in Δrpo mutants and mutants with lesions in PEP function (Hess et al., 1993; Allison et al., 1996; Hajdukiewicz et al., 1997; Silhavy and Maliga, 1998; De Santis-Maciossek et al., 1999; Krause et al., 2000; Legen et al., 2002), we observe the accumulation of larger amounts of not properly processed transcripts. Primer extension analyses indicate that either the transcriptional activity of the PEP enzyme and/or the mRNA stability of plastid genes are affected in the mutants. Since *atpB* mRNA levels and transcription rates are not downregulated in the *ptac2* mutants (Figures 8 and 9), it is likely that the lower signal at the PEP promoter site of *atpB* is specific for the PEP activity. We have chosen the *atpB* gene for this study because the transcript level for this gene is comparable in mutant and wild-type seedlings. A more detailed analysis of NEP and PEP promoter site usages in the *ptac* mutants requires a better knowledge of the exact initiation sites of plastid genes in *Arabidopsis*.

Proper expression of plastid genes is essential for the differentiation of proplastids to chloroplasts (Baumgartner et al., 1993; Mache et al., 1997). Hence, defects in plastid gene expression lead to reduced chlorophyll levels and obviously counteract any adverse effects, such as the assembly of thylakoid structures. However, electron micrographs of chloroplasts from wild-type and *ptac2*, *-6*, and *-12* plants (Figure 5) reveal abnormal membrane structure in mutant plants. This is in accordance with the observation of reduced photochemical efficiency (Table 4) in *ptac2*, *-6*, and *-12* plants, allowing them to grow only under heterotrophic conditions. The *ptac* mutants investigated are phenotypically very similar to PEP-deficient tobacco mutants. Both contain undeveloped plastids that have vesiculated internal membranes instead of thylakoids, depending on the stage of the leaf (De Santis-Maciossek et al., 1999). Furthermore, several other mutants affected in plastid gene expression also have severe lesions in chloroplast development (Shirano et al., 2000; Ishizaki et al., 2005).

PTAC2, -6, and -12 exhibit no obvious sequence similarities to other known proteins from prokaryotic organisms, except that pTAC2 contains PPR and TPR motifs, which are characteristic for proteins involved in mRNA processing, stability, and/or translation (Fisk et al., 1999; Boudreau et al., 2000; Yamazaki et al., 2004). Thus, these genes must have newly developed after the establishment of eukaryotism. Several lines of evidence support the idea that these proteins might be involved in plastid transcription/translation. Since *ptac2*, *-6*, and *ptac12* are expressed in cells with different types of plastids, the proteins should be involved in a more general plastid function. The PEP promoter activity of *atpB* is specifically downregulated in the mutants, while the NEP promoter in *clpP* is not (Figure 10). The same alterations in plastid gene expression are observed in etiolated and light-grown seedlings. Thus, neither a block in thylakoid biogenesis or photosynthesis nor photodamage causes the observed phenotype of the organelle and of the plants. The observations that *Arabidopsis* knockout lines for pTAC2, -6, and -12 exhibit the same phenotype as mutants with lesions in the core subunits of PEP strongly suggests that the three new nuclear-encoded proteins are intrinsic components of the plastid transcription machinery.

METHODS

Plant Material and Growth

Sinapis alba var Albatros and *Arabidopsis thaliana* (ecotype Columbia) were used for all studies. The T-DNA insertion lines (Salk_075736, Salk_024431, and Salk_025099) were obtained from NASC. *Arabidopsis* was grown on Murashige and Skoog medium (Murashige and Skoog, 1962) at 21°C with a day/night cycle of 16/8 h (50 to 60 μE m^{-2} s^{-1}; Osram LW30); if not, other light intensities are mentioned. For propagation, *Arabidopsis* seedlings were transferred to soil after 18 d, and the seeds were harvested in Aracon tubes (Beta Tech). For analysis of tissue-specific gene expression and biochemical studies, *Arabidopsis* and mustard plants were grown on soil in a growth chamber (day/night rhythm of 16/8 h; 80 to 100 μE m^{-2} s^{-1}, 21°C; Osram LW30).

Chlorophyll and Fluorescence Induction Measurements

Chlorophyll and fluorescence measurements were performed with 14-d-old *Arabidopsis* seedlings (5 to 10 μE m^{-2} s^{-1}; Osram LW30) grown on Murashige and Skoog medium. For fluorescence measurements, a Fluorcam 700 MF (Photon System Instruments) was used. After dark acclimation (15 min), the fluorescence were measured according to Wagner et al. (2005). The nomenclature of the standard chlorophyll parameters refer to van Kooten and Snel (1990). Chlorophyll and carotenoid pigments were determined by HPLC according to Büch et al. (1994). Samples were ground in liquid nitrogen in Eppendorf tubes and extracted as described by Ensminger et al. (2001).

Isolation of TAC

Chloroplasts were isolated from 2 to 3 kg cotyledons of 5-d-old mustard seedlings or 4-week-old *Arabidopsis* rosette leaves by sucrose gradient centrifugation (18 gradients at 35 mL; Tiller et al., 1991) at 4°C. After lyses of the chloroplasts in 200 mL buffer A (50 mM Tris-HCl, pH 7.6, 100 mM [NH$_4$]$_2$SO$_4$, 4 mM EDTA, 25% glycerol, 1% Triton X-100, 40 mM 2-mercaptoethanol, and 50 μg/mL phenylmethylsulfonyl fluoride [PMSF];

Rushlow and Hallick, 1982), the insoluble material was removed by centrifugation (20,000*g*, 4°C, 30 min).

Thirty microliters of the soluble fraction was used for gel filtration on several Sepharose 4B columns (2 cm diameter, 100 cm length, column volume 380 mL) at 4°C with buffer A. Fractions with transcriptional activity were combined and the TAC precipitated by ultracentrifugation (5 h, 200,000*g*, 4°C). The pellets were resuspended in 15 mL of buffer B (50 mM Tris-HCl, pH 7.6, 100 mM [NH$_4$]$_2$SO$_4$, 4 mM EDTA, 25% glycerol, 40 mM 2-mercaptoethanol, and 50 μg/mL PMSF), the insoluble material removed by centrifugation (10 min, 20,000*g*, 4°C), and the soluble proteins applied to a Sepharose 2B column (diameter 1.5 cm, length 170 cm, and volume 301 mL). After elution of the transcriptional active fractions with buffer B, the TAC was obtained by ultracentrifugation as described above. Final resuspension occurred in 1 mL of buffer C (50 mM Tris-HCl, pH 7.6, 50 mM [NH$_4$]$_2$SO$_4$, 4 mM EDTA, 10% glycerol, 40 mM 2-mercaptoethanol, and 50 μg/mL PMSF). Alternatively, the eluate of the first column was subjected to either Heparin Sepharose CL-6B or Q Sepharose chromatography. After resuspension of the TAC in 50 mM Tris-HCl, pH 7.6, 50 mM [NH$_4$]$_2$SO$_4$, 5 mM MgCl$_2$; 10% glycerol, 40 mM 2-mercaptoethanol, and 50 μg/mL PMSF, and DNase/RNase treatment at 37°C for 1 h, it was loaded onto a Heparin Sepharose CL-6B column (diameter 1.0 cm, length 10 cm, and volume 7 mL). The proteins were eluted with 50 mM Tris-HCl, pH 7.6, 2 M [NH$_4$]$_2$SO$_4$, 10% glycerol, 4 mM EDTA, 40 mM 2-mercaptoethanol, and 50 μg/mL PMSF, dialyzed and concentrated against the buffer C, and used for MS. For Q Sepharose chromatography (diameter 1.0 cm, length 10 cm, and volume 7 mL), the DNase/RNase treatment was omitted.

Transcription Assay

In vitro transcription was analyzed by measuring [^{3}H]UTP incorporation into RNA under conditions as described by Reiss and Link (1985). One unit was defined as incorporation of 1 fmol [^{3}H] into UTP in 30 min at 30°C (Suck et al., 1996).

Preparation of Samples and MS

After phenol/chloroform extraction of the transcriptionally active fraction, proteins were precipitated with ethanol, dried, and resuspended in 50 μL 50 mM NH$_4$HCO$_3$ and 0.05% β-dodecylmaltoside. After denaturation (95°C for 10 min), proteins were digested with trypsin according to manufacturer's instructions (Promega) at 37°C for 16 h. The peptides were then purified with POROS-R2 (Applied Biosystems) on a C18 Zip-Tip column (Millipore; Stauber et al., 2003). Silver-stained bands from protein gels were analyzed according to Stauber et al. (2003). MS and MS/MS spectra were recorded with a LCQ Deca XP IONTRAP mass spectrometer (Thermo) equipped with a nano-HPLC system (Ultimate; Dionex) according to Stauber et al. (2003). Liquid chromatography was performed with a reverse-phase column (PepMap C18 column; LC-Packings, Dionex). Identification of the proteins occurred with the Finnigan Sequest/Turbo Sequest software (revision 2.0; ThermoQuest) by comparing the recorded masses with those calculated for trypsin digestion products of all *Arabidopsis* peptides available in the databases (ftp://ftp.arabidopsis.org/sequences/blast_datasets/; The Arabidopsis Information Resource).

Array Hybridization and Quantification

Theme-specific plastome macroarrays were produced by spotting gene-specific PCR products of all 78 plastome-encoded proteins (100 to 500 bp in length, amplified from the 3′ end of the cDNA) in duplicates on Hybond N$^+$ membranes (Amersham Pharmacia Biotech). DIG-labeled cDNA of the wild type and mutants were synthesized from 5 μg of RNA and

quantified as described by Kandlbinder et al. (2004). Each cDNA from three independent experiments was hybridized with an array filter of the plastome macroarrays. Array hybridization and data evaluation were performed as described in detail by Kandlbinder et al. (2004). The spot intensities were quantified with AIDA Array Vision software (Raytest) and normalized according to whole intensity of all spots on the array. Data management excluded all spots that gave signal intensities below 120% of the background or whose signals varied >50% in duplicates in at least one experiment. The normalized spot intensities were tested for each treatment against the wild type by the use of Student's t test analysis (P < 0.05, P < 0.1, and P < 0.2). To quantify differential expression of the mutant lines, IF was calculated by the ratio of the average normalized signal intensities of the mutant lines and the wild type.

Real-Time PCR

Real-time quantitative RT-PCR was performed using an iCycler iQ real-time PCR detection system and iCycler software version 2.2 (Bio-Rad). Total RNA was isolated from three independent replicates of seedlings. For the amplification of PCR products, iQ SYBR Green Supermix (Bio-Rad) was used according to the manufacturer's protocol in a final volume of 25 μL. The iCycler was programmed to 95°C 2 min; 40 × (95°C 30 s, 55°C 40 s, 72°C 45 s), 72°c 10 min followed by a melting curve program (55 to 95°C in increasing steps of 0.5°C). All reactions were performed in triplicate. The mRNA levels for each cDNA probe were normalized with respect to the actin mRNA level. Fold induction values of target genes were calculated with the ΔΔCP equation of Pfaffl (2001) and related to the mRNA level of target genes in cotyledons, which was defined as 1.0.

Primer Extension Analysis

Seedlings were either kept in low light (5 to 10 μE m^{-2} s^{-1}; Osram LW30) or 3-d-old low-light grown seedlings were transferred to darkness for an additional 18 d. Primer extension reactions were performed with 10 μg of total leaf RNA according to standard protocols (Sambrook et al., 1989). Briefly, primer PE3AthatpB (5′-CGGTTATGCGTCCCATTTATTCATC-3′; position 54,537) and PE104Ath*clpP* (5′-GGTACTTTTGGAACGCCAA-TAGGC-3′; position 71,857) were end-labeled with [γ-32P]-ATP and T4 polynucleotide kinase. Primer extensions were performed using Super-script III MMLV reverse transcriptase (Gibco BRL) at 55°C and the resulting products analyzed on 5% sequencing gels. DNA sequences were generated by sequencing plasmid pMS2 and pMS3 using the same primer. Plasmid pMS2 harbors the *Arabidopsis rbcL-atpB* intergenic region (position 54,079 to 55,090), and pMS3 contains the *Arabidopsis clpP* upstream region (position 71,774 to 72,897; M. Swiatecka and K. Liere, unpublished data).

Run-On Transcription

Run-on assays were performed with 2 × 10^7 chloroplasts isolated from 12 g of leaves of 24-d-old plants in 100 μL of 50 mM Hepes-KOH, pH 8.0, 33 mM KCl, 10 mM MgCl$_2$, 125 μM ATP, 125 μM CTP, 125 μM GTP, 10 μM UTP, 50 μCi α-32P-UTP (110 TBq/mmol), and 55 μg heparin (Mullet and Klein, 1987). Incorporation of α-^{32}P-UTP into RNA was determined according to Rushlow and Hallick (1982). Four picomoles plasmid DNA, denatured in 0.5 M NaOH, was immobilized on nylon membranes and hybridized to the radiolabeled transcripts. Analyses occurred with the Storm PhosphorImager (Molecular Dynamics).

Miscellaneous

Methods not specified here were performed as described by Sambrook et al. (1989). The following primers were used for the amplification of genomic or plastid DNA fragments from wild-type or knockout lines (SALK) or for cDNA fragments: left border of inserted T-DNA in the SALK lines, 5′-TGGTTCACGTAGTGGGCCATCG-3′; Salk_075736-f, 5′-TGT-TTATGGGAAGACGGAGAG-3′; Salk_075736-r, 5′-GGTCGCATTATG-TGCCAGC-3′; Salk_024431-f, 5′-ATGGCGTCTTCCGCCGCTTCTC-3′; Salk_024431-r, 5′-GATGTGCAATGAGTGACTATGGATG-3′; Salk_025099-f, 5′-GCGGTTATGGATTTCAGAGGACC-3′; Salk_025099-r, 5′-GAAGAGG-AGACTGATCCTTAA-3′; ptac2-3f, 5′-AAGCGTGGACTTTTCCCTGAG-3′; At1g74850-r, 5′-TTAAGCTGTGCTCCCTGCTAGTTCTT-3′; ptac6-2f, 5′-ACCGGAACAGAAGGACAAACG-3′; At1g21600-r, 5′-TTCAGTGTCT-CAAATTGGTTCTAG-3′; ptac12-2f, 5′-CAAAAGAGAAAACCGAGCAGC-3′; At2g34640-r, 5′-TTAAGGATCAGTCTCCTCTTC-3′; actin-f, 5′-GGT-AACATTGTGCTCAGTGGTGG-3′; actin-r, 5′-CTCGGCCTTGGAGATC-CACATC-3′; accD-f, 5′-TGGATAGTTTTGCTCCTGGTGA-3′; accD-r, 5′-TCACGAATCTTTCCGCTTTCA-3′; clpP-f, 5′-CCTGGAGAAGGAGA-TACATCTTGG-3′; clpP-r, 5′-CTTGGGCTTCTGTTGCTGAC-3′; atpA-f, 5′-TGGTAACCATTAGAGCCGACG-3′; atpA-r, 5′-CGACGATTGGTAAG-GCAGTCA-3′; atpB-f, 5′-GACGTATCGCCCAAATCATTG-3′; atpB-r, 5′-CGCTGGATAGATACCTTTGGCA-3′; ndhB-f, 5′-CTTCAGCTTCAGC-CACTCGAA-3′; ndhB-r, 5′-CAATCGCAATAATCGGGTTCA-3′; ndhF-f, 5′-TCCTTTTTCCGACAGCAACAA-3′; ndhF-r, 5′-CTCCATGGCATCAG-GTAACCA-3′; rbcL-f, 5′-GTATGGACGTCCCCTATTAGGATG-3′; rbcL-r, 5′-GGTAGTGAGACCCAATCTTGAGTG-3′; rps14-f, 5′-TCATTTGATTC-GTCGATCCTCA-3′; rps14-r, 5′-AACCATTTCCCGAAGGATGTG-3′; ycf3-f, 5′-ATGTCGGCTCAATCTGAAGGA-3′; ycf3-r; 5′-CGGTAATGACAGAT-CACAGCCA-3′. Insertions were checked by amplifying DNA fragments with gene-specific and T-DNA–specific primers. After cloning into the pGem-T vector, the insertions were sequenced. For RNA gel blot analyses and macroarray analyses, total RNA from 18-d-old wild-type or mutant plants or the tissue indicated in the figure was isolated with Trizol reagent (Gibco BRL). Etiolated material (see above) was used for the results shown in Figure 9E. For RNA gel blot analyses, RNA was isolated according to Sambrook et al. (1989), and 15 μg was loaded per lane. RT-PCR was performed with RevertAid H Minus M-MuLV reverse tran-scriptase according to the manufacturer's instruction (MBI-Fermentas).

For the immunological detection of proteins on membranes, plant material was homogenized with liquid nitrogen and dissolved in a fivefold excess of homogenization buffer (50 mM Tris-HCl, pH 8.0, 10 mM EDTA, 2 mM EGTA, and 10 mM DTT). After separation of soluble and membrane-bound proteins by centrifugation (10 min, 17,000*g*), soluble proteins were precipitated with trichloroacetic acid and resuspended in gel loading buffer (100 mM NaCO$_3$, 50 mM DTT, and 10% saccharose). The pellet containing membrane proteins was resuspended in gel loading buffer. The primary antibodies used for protein gel blot analyses have been described (Stöckel and Oelmüller, 2004). All procedures of electron microscopy were also described (Kusnetsov et al., 1994).

Accession Numbers

Sequence data from this article can be found in the GenBank/EMBL data libraries under accession numbers listed in Table 2.

REFERENCES

Allison, L.A. (2000). The role of sigma factors in plastid transcription. Biochimie **82,** 537–548.

Allison, L.A., Simon, L.D., and Maliga, P. (1996). Deletion of *rpoB* reveals a second distinct transcription system in plastids of higher plants. EMBO J. **15,** 2802–2809.

Altschul, S.F., Madden, T.L., Schäffer, A.A., Zhang, J.H., Zhang, Z., Miller, W., and Lipman, D.J. (1997). Gapped BLAST and PSI-BLAST: A new generation of protein database search programs. Nucleic Acids Res. **25,** 3389–3402.

Apweiler, R., et al. (2001). The InterPro database, an integrated documentation resource for protein families, domains and functional sites. Nucleic Acids Res. **29,** 37–40.

Aravind, L., and Koonin, E.V. (2000). SAP—A putative DNA-binding motif involved in chromosomal organization. Trends Biochem. Sci. **25,** 112–114.

Baginsky, S., Tiller, K., and Link, G. (1997). Transcription factor phosphorylation by a protein kinase associated with chloroplast RNA polymerase from mustard (*Sinapis alba*). Plant Mol. Biol. **34,** 181–189.

Baginsky, S., Tiller, K., Pfannschmidt, T., and Link, G. (1999). PTK, the chloroplast RNA polymerase-associated protein kinase from mustard *Sinapis alba* L.), mediates redox control of plastid *in vitro* transcription. Plant Mol. Biol. **39,** 1013–1023.

Baumgartner, B.J., Rapp, J.C., and Mullet, J.E. (1993). Plastid genes encoding the transcription/translation apparatus are differentially transcribed early in barley (*Hordeum vulgare*) chloroplast development. Plant Physiol. **101,** 781–791.

Boni, I.V., Isaeva, D.M., Musychenko, M.L., and Tzareva, N.V. (1991). Ribosome-messenger recognition: mRNA target sites for ribosomal protein S1. Nucleic Acids Res. **19,** 155–162.

Boudreau, E., Nickelsen, J., Lemaire, S.D., Ossenbuhl, F., and Rochaix, J.D. (2000). The *Nac2* gene of *Chlamydomonas* encodes a chloroplast TPR-like protein involved in *psbD* mRNA stability. EMBO J. **19,** 3366–3376.

Briat, J.F., Laulhere, J.P., and Mache, R. (1979). Transcription activity of a DNA-protein complex isolated from spinach plastids. Eur. J. Biochem. **98,** 285–292.

Brown, D., and Gold, L. (1996). RNA replication by Q beta replicase: A working model. Proc. Natl. Acad. Sci. USA **93,** 11558–11562.

Büch, K., Stransky, H., Bigus, H.J., and Hager, A. (1994). Enhancement by artificial electron acceptors of thylakoid lumen acidification and zeaxanthin formation. J. Plant Physiol. **144,** 641–648.

Cahoon, A.B., Harris, F.M., and Stern, D.B. (2004). Analysis of developing maize plastids reveals two mRNA stability classes correlating with RNA polymerase type. EMBO Rep. **5,** 801–806.

Cannon, G.C., Ward, L.N., Case, C.I., and Heinhorst, S. (1999). The 68 kDa DNA compacting nucleoid protein from soybean chloroplasts inhibits DNA synthesis in vitro. Plant Mol. Biol. **39,** 835–845.

Casano, L.M., Martin, M., and Sabater, B. (2001). Hydrogen peroxide mediates the induction of chloroplastic Ndh complex under photooxidative stress in barley. Plant Physiol. **125,** 1450–1458.

Chi-Ham, C.L., Keaton, M.A., Cannon, G.C., and Heinhorst, S. (2002). The DNA-compacting protein DCP68 from soybean chloroplasts is ferredoxin:sulfite reductase and co-localizes with the organellar nucleoid. Plant Mol. Biol. **49,** 621–631.

Cho, H.S., Lee, S.S., Kim, K.D., Hwang, I., Lim, J.S., Park, Y.I., and Pai, H.S. (2004). DNA gyrase is involved in chloroplast nucleoid partitioning. Plant Cell **16,** 2665–2682.

da Costa e Silva, O., Lorbiecke, R., Garg, P., Müller, L., Wassmann, M., Lauert, P., Scanlon, M., Hsia, A.P., Schnable, P.S., Krupinska, K., and Wienand, U. (2004). The *Etched1* gene of *Zea mays* (L.)

encodes a zinc ribbon protein that belongs to the transcriptionally active chromosome (TAC) of plastids and is similar to the transcription factor TFIIS. Plant J. **38,** 923–939.

Demmig-Adams, B., and Adams, W.W. (2002). Antioxidants in photosynthesis and human nutrition. Science **298,** 2149–2153.

De Santis-Maciossek, G., Kofer, W., Bock, A., Schoch, S., Maier, R.M., Wanner, G., Rudiger, W., Koop, H.U., and Herrmann, R.G. (1999). Targeted disruption of the plastid RNA polymerase genes rpoA, B and C1: Molecular biology, biochemistry and ultrastructure. Plant J. **18,** 477–489.

Desveaux, D., Allard, J., Brisson, N., and Sygusch, J. (2002). Crystallization and preliminary X-ray crystallographic analysis of p24, a component of the potato nuclear factor PBF-2. Acta Crystallogr. D Biol. Crystallogr. **58,** 296–298.

Desveaux, D., Subramaniam, R., Despres, C., Mess, J.N., Levesque, C., Fobert, P.R., Dangl, J.L., and Brisson, N. (2004). A "Whirly" transcription factor is required for salicylic acid-dependent disease resistance in Arabidopsis. Dev. Cell **6,** 229–240.

Draper, D.E., and Reynaldo, L.P. (1999). RNA binding strategies of ribosomal proteins. Nucleic Acids Res. **27,** 381–388.

Emanuelsson, O., Nielsen, H., Brunak, S., and von Heijne, G. (2000). Predicting subcellular localization of proteins based on their N-terminal amino acid sequence. J. Mol. Biol. **300,** 1005–1016.

Ensminger, I., Xyländer, M., Hagen, C., and Braune, W. (2001). Strategies providing success in a variable habitat: III. Dynamic control of photosynthesis in *Cladophora glomerata.* Plant Cell Environ. **24,** 769–779.

Fernandez-Silva, P., Martinez-Azorin, F., Micol, V., and Attardi, G. (1997). The human mitochondrial transcription termination factor (mTERF) is a multizipper protein but binds to DNA as a monomer, with evidence pointing to intramolecular leucine zipper interactions. EMBO J. **16,** 1066–1079.

Fisk, D.G., Walker, M.B., and Barkan, A. (1999). Molecular cloning of the maize gene *crp1* reveals similarity between regulators of mitochondrial and chloroplast gene expression. EMBO J. **18,** 2621–2630.

Gruissem, W., Narita, J.O., Greenberg, B.M., Prescott, D.M., and Hallick, R.B. (1983). Selective in vitro transcription of chloroplast genes. J. Cell. Biochem. **22,** 31–46.

Hajdukiewicz, P.T.J., Allison, L.A., and Maliga, P. (1997). The two RNA polymerases encoded by the nuclear and the plastid compartments transcribe distinct groups of genes in tobacco plastids. EMBO J. **16,** 4041–4048.

Hedtke, B., Börner, T., and Weihe, A. (1997). Mitochondrial and chloroplast phage-type RNA polymerases in *Arabidopsis.* Science **277,** 809–811.

Hedtke, B., Börner, T., and Weihe, A. (2000). One RNA polymerase serving two genomes. EMBO Rep. **1,** 435–440.

Hess, W.R., Prombona, A., Fieder, B., Subramanian, A.R., and Börner, T. (1993). Chloroplast *rps15* and the *rpoB/C1/C2* gene cluster are strongly transcribed in ribosome deficient plastids: Evidence for a functioning non-chloroplast-encoded RNA polymerase. EMBO J. **12,** 563–571.

Homann, A., and Link, G. (2003). DNA-binding and transcription characteristics of three cloned sigma factors from mustard (*Sinapis alba* L.) suggest overlapping and distinct roles in plastid gene expression. Eur. J. Biochem. **270,** 1288–1300.

Hu, J., and Bogorad, L. (1990). Maize chloroplast RNA polymerase: The 180-, 120-, and 38-kilodalton polypeptides are encoded in chloroplast genes. Proc. Natl. Acad. Sci. USA **87,** 1531–1535.

Igloi, G.L., and Kössel, H. (1992). The transcriptional apparatus of chloroplast. CRC Crit. Rev. Plant Sci. **10,** 525–558.

Ikeda, T.M., and Gray, M.W. (1999). Identification and characterization

of T7/T3 bacteriophage-like RNA polymerase sequences in wheat. Plant Mol. Biol. **40,** 567–578.

Ishizaki, Y., Tsunoyama, Y., Hatano, K., Ando, K., Kato, K., Shinmyo, A., Kobori, M., Takeba, G., Nakahira, Y., and Shiina, T. (2005). A nuclear-encoded sigma factor, Arabidopsis SIG6, recognizes sigma-70 type chloroplast promoters and regulates early chloroplast development in cotyledons. Plant J. **42,** 133–144.

Jeong, S.Y., Peffer, N., and Meier, I. (2004). Phosphorylation by protein kinase CKII modulates the DNA-binding activity of a chloroplast nucleoid-associated protein. Planta **219,** 298–302.

Jeong, S.Y., Rose, A., and Meier, I. (2003). MFP1 is a thylakoid-associated, nucleoid-binding protein with a coiled-coil structure. Nucleic Acids Res. **31,** 5175–5185.

Kandlbinder, A., Finkemeier, I., Wormuth, D., Hanitzsch, M., and Dietz, K.J. (2004). The antioxidant status of photosynthesizing leaves under nutrient deficiency: Redox regulation, gene expression and antioxidant activity in *Arabidopsis thaliana.* Physiol. Plant **120,** 63–73.

Kasai, K., Kawagishi-Kobayashi, M., Teraishi, M., Ito, Y., Ochi, K., Wakasa, K., and Tozawa, Y. (2004). Differential expression of three plastidial sigma factors, OsSIG1, OsSIG2A, and OsSIG2B, during leaf development in rice. Biosci. Biotechnol. Biochem. **68,** 973–977.

Kato, Y., Murakami, S., Yamamoto, Y., Chatani, H., Kondo, Y., Nakano, T., Yokota, A., and Sato, F. (2004). The DNA-binding protease, CND41, and the degradation of ribulose-1,5-bisphosphate carboxylase/oxygenase in senescent leaves of tobacco. Planta **220,** 97–104.

Kimura, S., et al. (2002). A novel DNA polymerase homologous to *Escherichia coli* DNA polymerase I from a higher plant, rice (*Oryza sativa* L.). Nucleic Acids Res. **30,** 1585–1592.

Krause, G.H., and Weis, E. (1991). Chlorophyll fluorescence and photosynthesis: The basics. Annu. Rev. Plant Physiol. Plant Mol. Biol. **42,** 313–349.

Krause, K., Kilbienski, I., Mulisch, M., Rodiger, A., Schafer, A., and Krupinska, K. (2005). DNA-binding proteins of the Whirly family in *Arabidopsis thaliana* are targeted to the organelles. FEBS Lett. **579,** 3707–3712.

Krause, K., and Krupinska, K. (2000). Molecular and functional properties of highly purified transcriptionally active chromosomes from spinach chloroplasts. Physiol. Plant **109,** 188–195.

Krause, K., Maier, R.M., Kofer, W., Krupinska, K., and Herrmann, R.G. (2000). Disruption of plastid-encoded RNA polymerase genes in tobacco: Expression of only a distinct set of genes is not based on selective transcription of the plastid chromosome. Mol. Gen. Genet. **263,** 1022–1030.

Krupinska, K., and Falk, J. (1994). Changes in RNA polymerase activity during development and senescence of barley chloroplasts. Comparative analysis of transcripts synthesized either in run-on assays or by transcriptionally active chromosomes (TAC). J. Plant Physiol. **143,** 298–305.

Kusnetsov, V., Oelmüller, R., Sarwat, M.I., Porfirova, S.A., Cherepneva, G.N., Herrmann, R.G., and Kualeva, O.N. (1994). Cytokinins, abscisic acid and light affect accumulation of chloroplast proteins in *Lupinus luteus* cotyledons without notable effect on steady-state mRNA levels. Specific protein response to light/phytohormone interaction. Planta **194,** 318–327.

Kyrpides, N.C., Woese, C.R., and Ouzounis, C.A. (1996). KOW: A novel motif linking a bacterial transcription factor with ribosomal proteins. Trends Biochem. Sci. **21,** 425–436.

Legen, J., Kemp, S., Krause, K., Profanter, B., Herrmann, R.G., and Maier, R.M. (2002). Comparative analysis of plastid transcription profiles of entire plastid chromosomes from tobacco attributed to wild-type and PEP-deficient transcription machineries. Plant J. **31,** 171–188.

Lerbs-Mache, S. (1993). The 110-kDa polypeptide of spinach plastid DNA-dependent RNA polymerase: Single-subunit enzyme or catalytic core of multimeric enzyme complexes? Proc. Natl. Acad. Sci. USA **90,** 5509–5513.

Li, K., Pasternak, C., Hartig, E., Haberzettl, K., Maxwell, A., and Klug, G. (2004). Thioredoxin can influence gene expression by affecting gyrase activity. Nucleic Acids Res. **32,** 4563–4575.

Liere, K., Kaden, D., Maliga, P., and Börner, T. (2004). Overexpression of phage-type RNA polymerase RpoTp in tobacco demonstrates its role in chloroplast transcription by recognizing a distinct promoter type. Nucleic Acids Res. **32,** 1159–1165.

Liere, K., and Maliga, P. (1999). In vitro characterization of the tobacco *rpoB* promoter reveals a core sequence motif conserved between phage-type plastid and plant mitochondrial promoters. EMBO J. **18,** 249–257.

Loschelder, H., Homann, A., Ogrzewalla, K., and Link, G. (2004). Proteomics-based sequence analysis of plant gene expression– The chloroplast transcription apparatus. Phytochemistry **65,** 1785–1793.

Lurin, C., et al. (2004). Genome-wide analysis of *Arabidopsis* pentatricopeptide repeat proteins reveals their essential role in organelle biogenesis. Plant Cell **16,** 2089–2103.

Mache, R., Zhou, D.X., Lerbs-Mache, S., Harrak, H., Villain, P., and Gauvin, S. (1997). Nuclear control of early plastid differentiation. Plant Physiol. Biochem. **35,** 199–203.

Meurer, J., Plücken, H., Kowallik, K.V., and Westhoff, P. (1998). A nuclear-encoded protein of prokaryotic origin is essential for the stability of photosystem II in *Arabidopsis thaliana.* EMBO J. **17,** 5286–5297.

Morden, C.W., Wolfe, K.H., dePamphilis, C.W., and Palmer, J.D. (1991). Plastid translation and transcription genes in a non-photosynthetic plant: Intact, missing and pseudo genes. EMBO J. **10,** 3281–3288.

Moreira, D., and Philippe, H. (1999). Smr: A bacterial and eukaryotic homologue of the C-terminal region of the MutS2 family. Trends Biochem. Sci. **24,** 298–300.

Mullet, J.E., and Klein, R.R. (1987). Transcription and RNA stability are important determinants of higher plant chloroplast RNA levels. EMBO J. **6,** 1571–1579.

Murakami, S., Kondo, Y., Nakano, T., and Sato, F. (2000). Protease activity of CND41, a chloroplast nucleoid DNA-binding protein, isolated from cultured tobacco cells. FEBS Lett. **468,** 15–18.

Murashige, T., and Skoog, F. (1962). A revised medium for rapid growth and bioassays with tobacco tissue culture. Physiol. Plant **15,** 473–497.

Narita, J.O., Rushlow, K.E., and Hallick, R.B. (1985). Characterization of a *Euglena gracilis* chloroplast RNA polymerase specific for ribosomal RNA genes. J. Biol. Chem. **260,** 11194–11199.

Ogrzewalla, K., Piotrowski, M., Reinbothe, S., and Link, G. (2002). The plastid transcription kinase from mustard (*Sinapis alba L.*). A nuclear-encoded CK2-type chloroplast enzyme with redox-sensitive function. Eur. J. Biochem. **269,** 3329–3337.

Oleskina, Yu.P., Yurina, N.P., Odintsova, T.I., Egorov, T.A., Otto, A., Wittmann-Liebold, B., and Odintsova, M.S. (1999). Nucleoid proteins of pea chloroplasts: Detection of a protein homologous to ribosomal protein. Biochem. Mol. Biol. Int. **47,** 757–763.

Oswald, O., Martin, T., Dominy, P.J., and Graham, I.A. (2001). Plastid redox state and sugars: Interactive regulators of nuclear-encoded photosynthetic gene expression. Proc. Natl. Acad. Sci. USA **98,** 2047–2052.

Pasternak, C., Haberzettl, K., and Klug, G. (1999). Thioredoxin is involved in oxygen-regulated formation of the photosynthetic apparatus of *Rhodobacter sphaeroides.* J. Bacteriol. **181,** 100–106.

Pfaffl, M.W. (2001). A new mathematical model for relative quantification in real-time RT-PCR. Nucleic Acids Res. **29,** 2002–2007.

Pfannschmidt, T., and Link, G. (1994). Separation of two classes of plastid DNA-dependent RNA polymerases that are differentially expressed in mustard (*Sinapis alba* L.) seedlings. Plant Mol. Biol. **25,** 69–81.

Pfannschmidt, T., Ogrzewalla, K., Baginsky, S., Sickmann, A., Meyer, H.E., and Link, G. (2000). The multisubunit chloroplast RNA polymerase A from mustard (*Sinapis alba* L.). Integration of a prokaryotic core into a larger complex with organelle-specific functions. Eur. J. Biochem. **267,** 253–261.

Rajashekar, V.K., Sun, E., Meeker, R., Wu, B.W., and Tewari, K.K. (1991). Highly purified pea chloroplast RNA polymerase transcribes both rRNA and mRNA genes. Eur. J. Biochem. **195,** 215–228.

Reece, R.J., and Maxwell, A. (1991). DNA gyrase: Structure and function. Crit. Rev. Biochem. Mol. Biol. **26,** 335–375.

Reiss, T., and Link, G. (1985). Characterization of transcriptionally active DNA-protein complexes from chloroplasts and etioplasts of mustard (*Sinapis alba* L.). Eur. J. Biochem. **148,** 207–212.

Robinson, N.J., Procter, C.M., Connolly, E.L., and Guerinot, M.L. (1999). A ferric-chelate reductase for iron uptake from soils. Nature **397,** 694–697.

Rushlow, K.E., and Hallick, R.B. (1982). The isolation and purification of a transcriptionally active chromosome from chloroplast of *Euglena gracilis.* In Methods in Chloroplast Molecular Biology, M. Edelman, R.B. Hallick, and N.-H. Chua, eds (Amsterdam: Elsevier), pp. 543–550.

Sambrook, J., Fritsch, E.F., and Maniatis, T. (1989). Molecular Cloning: A Laboratory Manual. (Cold Spring Harbor, NY: Cold Spring Harbor Laboratory Press).

Sato, N., Albrieux, C., Joyard, J., Douce, R., and Kuroiwa, T. (1993). Detection and characterization of a plastid envelope DNA-binding protein which may anchor plastid nucleoids. EMBO J. **12,** 555–561.

Schürmann, P., and Jacquot, J.P. (2000). Plant thioredoxin systems revisited. Annu. Rev. Plant Physiol. Plant Mol. Biol. **51,** 371–400.

Sekine, K., Hase, T., and Sato, N. (2002). Reversible DNA compaction by sulfite reductase regulates transcriptional activity of chloroplast nucleoids. J. Biol. Chem. **277,** 24399–24404.

Shirano, Y., et al. (2000). Chloroplast development in *Arabidopsis thaliana* requires the nuclear-encoded transcription factor sigma B. FEBS Lett. **485,** 178–182.

Silhavy, D., and Maliga, P. (1998). Mapping of promoters for the nucleus-encoded plastid RNA polymerase (NEP) in the *iojap* maize mutant. Curr. Genet. **33,** 340–344.

Squires, C.L., and Zaporojets, D. (2000). Proteins shared by the transcription and translation machines. Annu. Rev. Microbiol. **54,** 775–798.

Sriraman, P., Silhavy, D., and Maliga, P. (1998). The phage-type PclpP-53 plastid promoter comprises sequences downstream of the transcription initiation site. Nucleic Acids Res. **26,** 4874–4879.

Stauber, E.J., Fink, A., Markert, C., Kruse, O., Johanningmeier, U., and Hippler, M. (2003). Proteomics of *Chlamydomonas reinhardtii* light-harvesting proteins. Eukaryot. Cell **5,** 978–994.

Stöckel, J., and Oelmüller, R. (2004). A novel protein for photosystem I biogenesis. J. Biol. Chem. **12,** 10243–10251.

Suck, R., Zeltz, P., Falk, J., Acker, A., Kossel, H., and Krupinska, K. (1996). Transcriptionally active chromosomes (TACs) of barley chloroplasts contain the alpha-subunit of plastome-encoded RNA polymerase. Curr. Genet. **30,** 515–521.

Summer, H., Pfannschmidt, T., and Link, G. (2000). Transcripts and sequence elements suggest differential promoter usage within the *ycf3-psaAB* gene cluster on mustard (*Sinapis alba L.*) chloroplast DNA. Curr. Genet. **37,** 45–52.

Suzuki, J.Y., Jimmy Ytterberg, A., Beardslee, T.A., Allison, L.A., Wijk, K.J., and Maliga, P. (2004). Affinity purification of the tobacco plastid RNA polymerase and in vitro reconstitution of the holoenzyme. Plant J. **40,** 164–172.

Tiller, K., Eisermann, A., and Link, G. (1991). The chloroplast transcription apparatus from mustard (*Sinapis alba* L.). Evidence for three different transcription factors which resemble bacterial sigma factors. Eur. J. Biochem. **198,** 93–99.

van Kooten, O., and Snel, J.F.H. (1990). The use of chlorophyll fluorescence nomenclature in plant stress physiology. Photosynth. Res. **25,** 147–150.

Wagner, R., Fey, V., Borgstädt, R., Kruse, O., and Pfannschidt, T. (2005). Screening for *Arabidopsis thaliana* mutants deficient in acclimatory long-term to varying light qualities using chlorophyll fluorescence imaging. Photosynthesis: Fundamental aspects to global perspectives. In Proceedings of the 13th International Congress of Photosynthesis, A. van der Est and D. Bruce, eds (Montreal, Canada: Allen Press), pp. 693–696.

Weihe, A., Hedtke, B., and Börner, T. (1997). Cloning and characterization of a cDNA encoding a bacteriophage-type RNA polymerase from the higher plant *Chenopodium album.* Nucleic Acids Res. **25,** 2319–2325.

Yamazaki, H., Tasaka, M., and Shikanai, T. (2004). PPR motifs of the nucleus-encoded factor, PGR3, function in the selective and distinct steps of chloroplast gene expression in *Arabidopsis.* Plant J. **38,** 152–163.

Young, D.A., Allen, R.L., Harvey, A.J., and Lonsdale, D.M. (1998). Characterization of a gene encoding a single-subunit bacteriophage-type RNA polymerase from maize which is alternatively spliced. Mol. Gen. Genet. **260,** 30–37.

Zellars, M., and Squires, C.L. (1999). Antiterminator-dependent modulation of transcription elongation rates by NusB and NusG. Mol. Microbiol. **32,** 1296–1304.

Zengel, J.M., Mueckl, D., and Lindahl, L. (1980). Protein L4 of the *E. coli* ribosome regulates an eleven gene r-protein operon. Cell **21,** 523–535.